A market simulation methodology for the calibration of ORDC

Jacques Cartuyvels
Anthony Papavasiliou

July 29, 2021

Contents

1. Introduction

Scarcity pricing is the practice of pricing electricity above the incremental cost of energy production in power systems during periods of system scarcity. Such pricing can be rationalized by a number of economic drivers, including the participation of price-responsive demand in the market, as well as the accurate valuation of the value of reserve capacity to the system through operating reserve demand curves (ORDCs). In the present report we are concerned with the latter.

Scarcity pricing contributes towards the mitigation of the missing money problem. As such, the analysis of the mechanism has been of interest to the Belgian regulatory authority of energy. In a series of studies, the Center for Operations Research and Econometrics (CORE) of UCLouvain and the CREG have published a number of reports for analyzing the mechanism, understanding its impact on the Belgian market, and proposing a series of measures for its implementation in Belgium. The focus of the present work is on the calibration of operating reserve demand curves, which are a key design parameter of the mechanism.

The analysis on the the role and incentives of operating reserve demand curves in a scarcity pricing scheme can either be performed in an *open* or *closed loop*. The open-loop approach is used in [ZZWT20] and [ELI18] in order to investigate variations of ORDC ex-post based on the historical levels of generation. Zarnikau in [ZZWT20] analyses the impact of a shift in the ORDC and its effect on the real-time market price and investment incentives for natural-gas-fired generation in the Texas electricity market. [ELI18] compare the level of the adder produced by 2 different assumptions regarding the eligibility of assets for scarcity pricing. The closed-loop approach in [ZB14] and [LMSA20] uses a short-term operating model for simulating the incentives induced by scarcity pricing. Zhou and Botterud propose an ORDC based on the loss of load probability that accounts for the wind, load and generation uncertainty in [ZB14]. Lavin [LMSA20] introduces a LOLP as a function of the ambient temperature, in order to represent the higher probability of forced outage for generators under extreme temperature conditions.

1.1. The Role of ORDCs in Scarcity Pricing and our Methodology

Scarcity pricing essentially implements a real-time market for reserve. In such a market (as in day-ahead or other forward markets for reserve), the transmission system operator procures reserve capacity on behalf of system users in order to ensure the reliable operation of the system. Operating reserve demand curves determine the equilibrium price of reserve. Since energy and reserve prices are inherently linked by a no-arbitrage condition which dictates that the price of energy is equal to the price of reserve plus the marginal cost of the marginal unit in the system, the price of reserve serves as an "adder" that creates a revenue stream for generators which exceeds the marginal cost of the marginal unit in the system. This revenue stream represents the value of flexibility in the system[1], and contributes to the mitigation of the missing money problem. Furthermore, this revenue stream can occur without requiring balancing service providers

[1]We will refer to flexibility in this report as automatic and manual frequency restoration reserves.

to submit supramarginal offers in the balancing market.

Scarcity prices based on ORDC reward balancing service providers that can either contribute to system availability by making their capacity available to the system in real time, or by responding to system imbalances through rapid variations of their output. The mechanism thus has an inherent built-in pay-for-performance property.

The reserve price, which is also referred to broadly as the "scarcity adder", is ultimately driven by the shape of the demand curve for reserve. All markets (including Belgium) have ORDCs, even those which use fixed or dynamic reserve requirements. Fixed reserve requirements simply imply a price-inelastic ORDC. Independent system operators such as ISO-NE, MISO, SPP and CAISO currently value operating reserves with stepped ORDCs, whereas ERCOT and PJM have implemented a downward sloping ORDC based on the loss of load probability (LOLP) and the value of lost load (VOLL) [NYI19]. It is worth noting that the market monitor of ISO-NE and MISO has recommended a transition to ORDCs based on LOLP and VOLL.

The anchoring of ORDCs on LOLP and VOLL is rationalized by Hogan [Hog13]. The starting point of Hogan's derivation is a two-stage stochastic program which represent an economic dispatch under uncertainty. The goal is to dispatch the system in a way that seeks an optimal tradeoff between the cost of operating the system and the expected cost of not serving load. The theory can be generalized to multiple reserve products that are substitutable as well as multiple zones [HP19].

The analysis of Hogan is an *approximation* of actual operations which is needed for establishing the connection between LOLP, VOLL, and the incremental value of reserve capacity in the system. The resulting ORDC depends on a number of design assumptions, and we investigate these assumptions in detail in the present work. In doing so, we adopt a methodology which is inspired by the spirit of Hogan's analysis: in deciding what are the appropriate design choices for an ORDC, we assess the performance of a given ORDC based on the tradeoff that this ORDC achieves between cost of operation and system reliability.

In order to understand the fundamental tradeoff, consider two extremes. At one extreme, over-valuing reserve capacity with an ORDC that is too wide implies exorbitant fixed costs of committing reserve and dispatvhing untis out of merit in order to ensure that the system is protected at all times. At the other extreme, a very narrow ORDC implies running the system with minimal reserves, but often without being able to serve demand, with exorbitant costs in terms of load shedding. A well-calibrated ORDC seeks the optimal tradeoff between these two extremes.

1.2. Contribution of Our Work and Structure of this Report

In this work we develop a detailed production simulation model of the Belgian electric power system which aims at quantifying the tradeoff between operating cost and reliable system operation, with the objective of fine-tuning the calibration of an ORDC for implementing scarcity pricing. The modeling contribution of our work is to extend the state of the art in production simulation models for the purpose of analyzing scarcity pricing.

The work presented here is inspired by the closed-loop modelling approach of [ZB14] and [LMSA20]. We extend the scope of their analysis by reducing the granularity from 1 hour to 7.5 minutes and by introducing interleaved modules to capture the dynamic adjustment of system operations to uncertainty and the lag of activation of reserves. Theses features allows us to asses scarcity pricing in practice and to account for the reality and constraints of balancing the market on imbalance period. The modelling precision of our model matches state-of-the-art models for simulating short-term operations, such as the Smart-ISO model developed by Simao and Powells [SPAK17] and the three-level scheduling model of [BSB$^+$15]. We also take a step back from the sophisticated representation of the LOLP in [LMSA20] to consider the parametrization of ORDCs.

Apart from the methodological novelty of our analysis, there is an important institutional element to the work. The current modeling effort is contributing directly to the implementation of a scarcity pricing mechanism in the Belgian electricity market. The results of the analysis constitute the basis for the recommendation of the Belgian regulatory authority for the rollout of scarcity pricing in Belgium.

The report is structured as follows. In section 2 we present our methodology and the ORDC variants that we consider in our work. The model used for our simulation is presented in section 3. In section 4 we present the data that we use in our simulator. Section 5 describes the validation of the simulator and section 6 presents the results of our analysis. We conclude and present directions of further research in section 7.

2. Description of the Problem

In this section we begin by describing how scarcity pricing can be implemented in Belgium and how it can accommodate different types of reserve. We then move to the focus of the analysis, which are the variants of ORDCs.

2.1. Implementation of Scarcity Pricing in Belgium

As described in the introduction, the marginal value of an additionnal MWh of balancing capacity is defined as a function of the *value of lost load* ($VOLL$) and the *loss of load probability* ($LOLP(\cdot)$) given the level of reserve in the system (r). This allows us to characterize the *operating reserve demand curve* (1):

$$V^R(r) = (VOLL - \widehat{\text{MC}}) \cdot LOLP(r) \tag{1}$$

Note that the term $\widehat{\text{MC}}$ is the marginal cost of the marginal technology in the system. The term ensures that there is no arbitrage opportunity between the energy and reserve market.

Depending on the degree to which a market is aligned with the co-optimization of energy and reserves, the ORDC takes on slightly different roles:

i. The most complete integration of scarcity pricing would correspond to the co-optimization of reserve and energy in real time. The ORDC would then be an explicit demand curve for reserve, which is inserted in the multi-product auction.

ii. In the absence of a co-optimization of energy and reserves, we could use the ORDC to compute *adders* based on the amount of leftover reserve in real time, as measured by system telemetry. This adder would be a price component that would be added to the real-time energy price (the balancing energy price, in EU nomenclature). The adder would correspond to the level of stress in the system.

In the context of implementing the mechanism in the Belgian market, the focus has been on the second approach. The adder computed by the formula above is (i) applied as an add-on to the balancing energy price, (ii) is applied as an add-on to the imbalance price, and (iii) is also used for the settlement of reserve imbalances, thus implementing a real-time market for reserve capacity.

2.2. Multiple Reserve Products

The formula presented in the previous section can be generalized to the case of multiple reserve products of different quality. The quality of reserve refers to the delivery time that is required for the specific balancing capacity product to be fully available. The authors in [PSdMd19] inspire themselves from the ERCOT design [ERC] to suggest the introduction of two ORDCs that would then be used for computing three adders for the Belgian market. The two ORDCs proposed are (i) the 7.5-minute ORDC (eq. (2)) which would be used for valuing balancing capacity that can be fully activated in 7.5 minutes

(which corresponds in our analysis to aFRR capacity) and (ii) the 15-minute ORDC (eq. (3)) which would be used for valuing balancing capacity that can be fully activated in 15 minutes (which corresponds in our analysis to mFRR capacity). The demand curves can be expressed as follows:

$$V_{7.5}^{R}(r_{7.5}) = \frac{1}{2} \cdot (VOLL - \widehat{\text{MC}}) \cdot LOLP_{7.5}(r_{7.5}) \tag{2}$$

$$V_{15}^{R}(r_{15}) = \frac{1}{2} \cdot (VOLL - \widehat{\text{MC}}) \cdot LOLP_{15}(r_{15}) \tag{3}$$

Here, $LOLP_x(\cdot)$ corresponds to the loss of load probability after x minutes, with r_x being the amount of reserve that can be activated within x minutes. The loss of load probability after x minutes is described in equation (4) and can be interpreted as the probability of the imbalance after x minutes exceeding the balancing capacity that can be made available in x minutes:

$$LOLP_x(r_x) = \mathbb{P}(imb_x \geq r_x) \quad \text{with } imb_x \sim \mathcal{N}(\mu_x, \sigma_x^2) \tag{4}$$

The imbalance is here assumed to be drawn from a normal distribution with mean μ_x and standard deviation σ_x estimated from the historical system imbalance of the system. These parameters are computed per 4-hour block and per season, in order to account for seasonality. The values of these parameters, as estimated for the Belgian market, can be found in table 4 of section 4.

The level of balancing capacity that can be made available after 15 minutes, r_{15}, is computed ex-post based on telemetry measurements. The value of $r_{7.5}$ is also computed ex-post, according to a pre-defined availability for 7.5 minutes, and the 15-minute telemetry data.

The adders that a generator is eligible for are then characterized by the capability of that generator to deliver balancing capacity in a given timeframe [2]

- The adder for 7.5-minute reserve capacity or *fast adder*:

$$\lambda^F = V_{7.5}^{R}(r_{7.5}) + V_{15}^{R}(r_{15}) \tag{5}$$

  This adder is paid to the standby (not activated) balancing capacity that can react in 7.5 minutes. Note that any generator eligible for the 7.5-minute adder would also be directly eligible for the 15-minute adder.

- The adder for 15-minute reserve capacity or *slow adder*:

$$\lambda^S = V_{15}^{R}(r_{15}) \tag{6}$$

  This adder is paid to the standby balancing capacity that can react in 15 minutes.

[2] Equations (5) and (6) are equal to the dual variables associated to the clearing constraint of fast and slow reserve, respectively, in the economic dispatch problem that co-optimizes energy and reserves. Equalizing the adder for energy to the fast reserve adder is an approximation of the dual variable associated to the clearing constraint of energy for the same economic dispatch problem. This proxy differs from the co-optimization adder when ramp constraints are binding. A discussion about this approximation can be found in the supplement of [PSdMd21].

- The adder for energy: This adder is paid in real time to any generator producing balancing energy, in addition to the balancing price. It is equal to the fast adder (5).

In ERCOT there is one adder for spinning reserve that can respond immediately and one adder for non-spinning reserve that can be made available in 30 minutes [ERC]. Thus, the underlying theory can be adapted for deriving formulas that are tailored to the specific reserve product definitions of different markets.

2.3. ORDC Variants

We now proceed to consider alternative assumptions that affect the parameters that are employed in the adder formulas of the previous sections. The three variations that we analyse in this work are differentiated by (i) different values for VOLL, (ii) whether the argument of the LOLP operator is the reserve capacity remaining before or after the activation of reserves in a given imbalance interval, and (iii) whether imbalance increments within an imbalance interval are assumed to be correlated or not.

The simulation platform that we put in place is able to quantify various metrics of performance that can be used for comparing the ORDC alternatives. The first metric of performance is the total cost of operation of the system. Another important metric is the resulting balancing energy and reserve price signal,

2.3.1. Variant 1: VOLL at 8300 versus VOLL at 13500

The value of loss of load has been estimated at 8300 €/MWh by the Belgian federal planning bureau [Dev17]. It has been used as the reference value of the VOLL in [PSdMd19]. The value of 13500 €/MWh has also been proposed by the CREG as an alternative value of the VOLL as it represents the current limit of the imbalance price.

The effect of the different choices of VOLL on the ORDC can be visualized in figure 1.

2.3.2. Variant 2: Computation of the Adder Before the Activation of Reserve versus After the Activation of Reserve

The second assumption that we test in our analysis is whether the reserve capacity which is used as an argument of LOLP corresponds to balancing capacity remaining before or after the activation of reserve within a given imbalance interval. These two variants will be referred to as *pre-activation* and *post-activation* for the remainder of the report.

The pre-activation variant discussed in this work corresponds more closely to the original model developed by Hogan in [Hog13]. In [PSdMd21], it is pointed out that the pre- and post-activation variants correspond to different interpretations of what would be implied in terms of system operator expectations by making a certain quantity of reserve available in real time: does 1 MW of reserve imply that a resource has been allowed time to recover from its balancing dispatch during the previous imbalance interval, or should the resource be prepared to offer this 1 MW even if it has not been afforded time

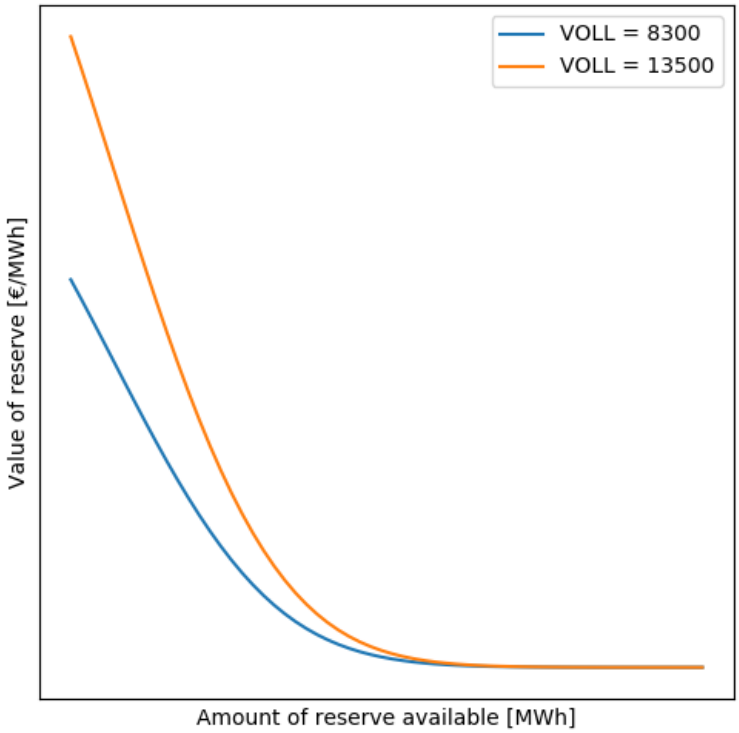

Figure 1: VOLL at 8300 €/MWh versus VOLL at 13500 €/MWh.

to return to its originally scheduled setpoint? The effect of the assumption is found to be significant in the context of the stochastic equilibrium formulation presented in [PSdMd21]. As the time step of the real-time / balancing market becomes shorter (5 minutes currently in the US, and 15 minutes in European), the distinction becomes less relevant.

If the post-activation reserve capacity margin is denoted as r, then the pre-activation margin is $r - imb$, with imb being the difference between the scheduled and actual demand. This allows us to value balancing capacity at the beginning of an interval before absorbing the imbalance. Figure 2 illustrates the impact of negative and positive imbalance on the pre-activation variant compared to the post-activation variant. An example can be found in appendix C.

2.3.3. Variant 3: Independent versus Correlated Distributions of 7.5-Minute Imbalance Increments

The third assumption relates to whether or not we assume that imbalance increments within an imbalance interval are assumed to be correlated or not. As explained in [Hog13], the scarcity pricing formulas for two reserve products, that are distinguished between fast and slow, is based on an analytical derivation of a two-stage stochastic

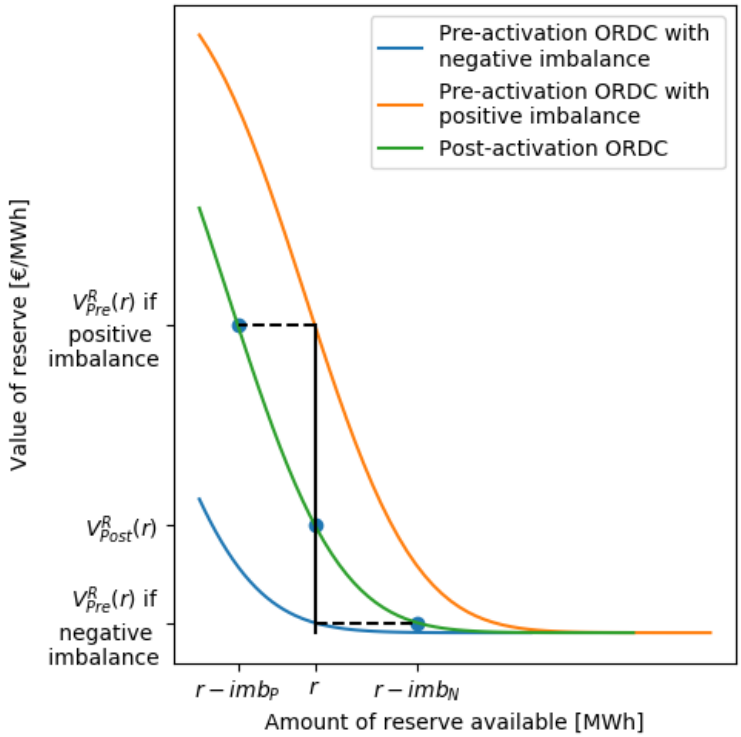

Figure 2: ORDC for pre-activation versus post-activation variants, for both positive and negative imbalances.

economic dispatch. In this stochastic economic dispatch model, fast reserve is assumed to be able to respond within the first and second interval, whereas slow reserve is assumed to only be able to respond in the second interval.

The question of independent versus correlated imbalance increments refers to how imbalance increments are assumed to behave in the first and second interval of this analytical framework. On the one extreme, the assumption of correlated imbalances implies that the total imbalance over both stages evolves linearly from the beginning to the end of the interval, and thus that imbalance increments are perfectly correlated. On the other extreme, the assumption of independent imbalances implies that the total imbalance over both stages is the sum of two independently distributed imbalance increments occurring at stages 1 and 2 respectively. The distinction is depicted graphically in figure 3, which is sourced from [PSB18].

The distinction affects the implied standard deviation of the imbalance that is used in the 7.5-minute version of formula (4). Concretely, for a given standard deviation of total imbalance σ, an assumption of independent increments implies a greater standard deviation for the imbalance increment that occurs in the first interval, during which fast capacity should response. Intuitively, this is due to the fact that high deviations in total should require more "noisy" imbalance increments, since independent imbalance

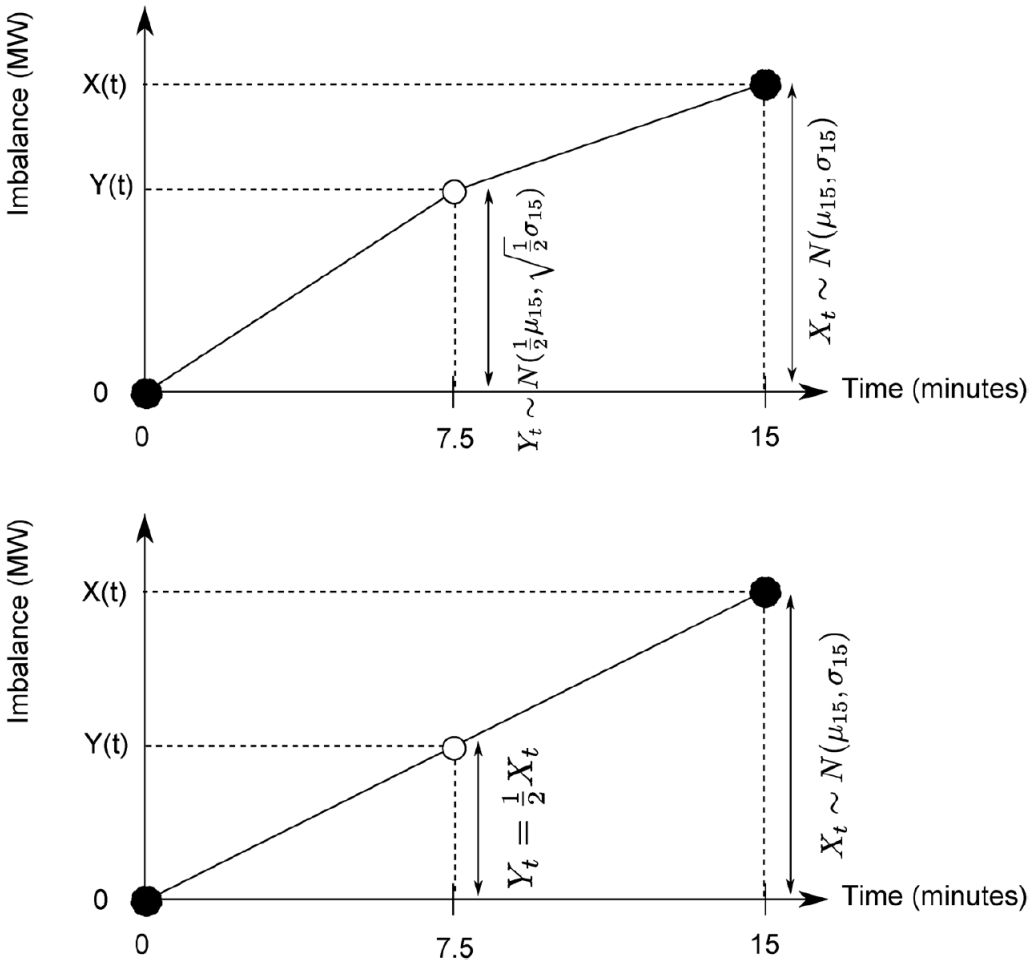

Figure 3: Independent (upper panel) and correlated (lower panel) imbalance increments

increments tend to cancel each other out. Thus, given σ for the 15-minute imbalance, this implies a standard deviation of $\sigma/\sqrt{2}$ for the 7.5-minute imbalance for the case of independent increments, versus $\sigma/2$ for the case of perfectly correlated increments. Thus, the level of the fast reserve adder in formula (5) is affected by this assumption. Regardless of the distribution of the imbalance increments, for a given mean of total imbalance μ, the 7.5 minutes imbalance increments' mean value is $\mu/2$.

In previous work [PSB18], we have examined this question based on historical imbalance data. In particular, we have used 1-minute imbalance data recorded by ELIA to uncover very strong correlations between consecutive 7.5-minute imbalance increments. In this work, we rather approach the question from the point of view of the impact of this assumption on the resulting fast ORDC.

3. The System Model

This section provides a detailed description of the simulator that we have implemented in order to compare the different ORDC design options. The simulator models an idealized, fully coordinated operation of the Belgian system, with a focus on real-time operation. It consists of 4 embedded optimization problems that are solved in sequence throughout the day, in a rolling window fashion. Each of these optimization problems is solved over varying scheduling windows and in a sequencing order that attempts to approximate the real-time operation of the system. Particular care is given to (i) the operational constraints of the individually modelled generation plants; (ii) the revelation of real-time uncertainty and the scheduling of the system based on forecast information; (iii) the effect of each decision-making stage on subsequent optimization problems.

The remainder of this section is composed of a description of the sequence of simulations and a thorough characterization of the four optimization problems: (i) the day-ahead unit commitment, (ii) the intermediate rolling-window unit commitment, (iii) the pre-real-time rolling-window unit commitment, and (iv) the real-time economic dispatch.

3.1. Sequence of Simulations

The simulator models the operation of a perfectly coordinated system, where a centralized optimization commits and dispatches in a coordinated fashion. Uncertainty is assumed to stem from the actual load that needs to be served by the system. The sequential optimization of system scheduling aims at replicating the real-time controllability of the different assets present in the system, with a specific focus on quantifying the interplay between lags in decision making and the revelation of uncertain information in the system. The purpose of the simulator is to quantify the fundamental tradeoff that ORDCs aim at balancing: incurring large fixed costs for committing flexible resources that can allow the system to operate reliably in real time, versus running the risk of not fully covering imbalances.

Depending on the characteristics of an asset, its commitment plan and dispatch decision will be obtained by different optimization problems. Assets can be partitioned into 3 broad categories, based on their real-time controllability.

1. **DA scheduled generators:** Certain generators are not able to modify their planned day-ahead dispatch. This might be caused by the inflexibility of their plant or a link between their electricity production and the production of other goods, such as heating. The electricity production of these generators is typically determined in forward processes, and these units are not participating in a balancing market.

2. **Fast balancing capacity:** CCGT generators constitute the bulk of this category. They require a non-negligible lag to start up (between 1 and 3 hours) but are very reactive once committed.

3. **Slow balancing capacity:** This category includes all emergency generators.

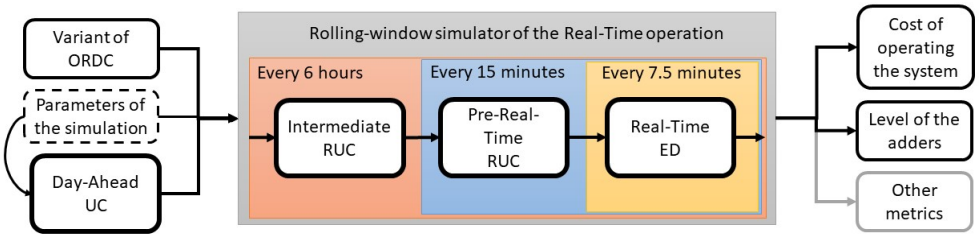

Figure 4: Sequence of optimization problems that are implemented in our system simulator.

These generators are typically costly to start up, but can be activated in a very short time, in order to free up some of the fast balancing capacity.

Note that generators can exist at the intersection between fast and slow balancing capacity. OCGT plants, for example, can provide fast balancing capacity once committed, or slow balancing capacity when shut down.

As stated previously, the simulator is based on 4 optimization problems that have different roles and whose dispatch and commitment decisions apply to a specific group of assets. The 4 optimization problems are, in ascending order of length of scheduling window, (i) the *day-ahead unit Commitment* (DA-UC), (ii) the *intermediate rolling window unit commitment* (Inter-RUC), (iii) the *pre-real-time rolling window unit commitment* (PRT-RUC) and (iv) the *real-time economic dispatch* (RT-ED). These models are sequenced as indicated in figure 4. Each of these problems is described hereunder.

- **The day-ahead unit commitment (DA-UC):** This problem is used for scheduling the inelastic production that will not vary in real time from its day-ahead set-point. the model is launched once, before the beginning of the day, with a scheduling horizon of 72 hours. The model assumes a fixed initial dispatch of units for the day, which will be identical for every variant of ORDC that is tested in our analysis. The parameters of the simulation include the day-ahead load forecast, as well as settings that determine the reactivity and availability of the generation pool. This problem also determines the target hydro storage target for the real-time models. The system is allowed to deviate from this target in order to address balancing issues, but such deviations are penalized.

- **The intermediate rolling-window unit commitment (Inter-RUC):** This problem is solved every six hours over a 24-hour scheduling window. The Inter-RUC determines the commitment of CCGT plants for the next 6 hours until the next Inter-RUC is launched. This process thus proxies an intraday market adjustments. It is costly to keep CCGT plants online, therefore an optimal scheduling of these plants requires a significant scheduling window.

- **The pre-real-time rolling-window unit commitment (PRT-RUC):** This problem determines the commitment of emergency generators. The model is

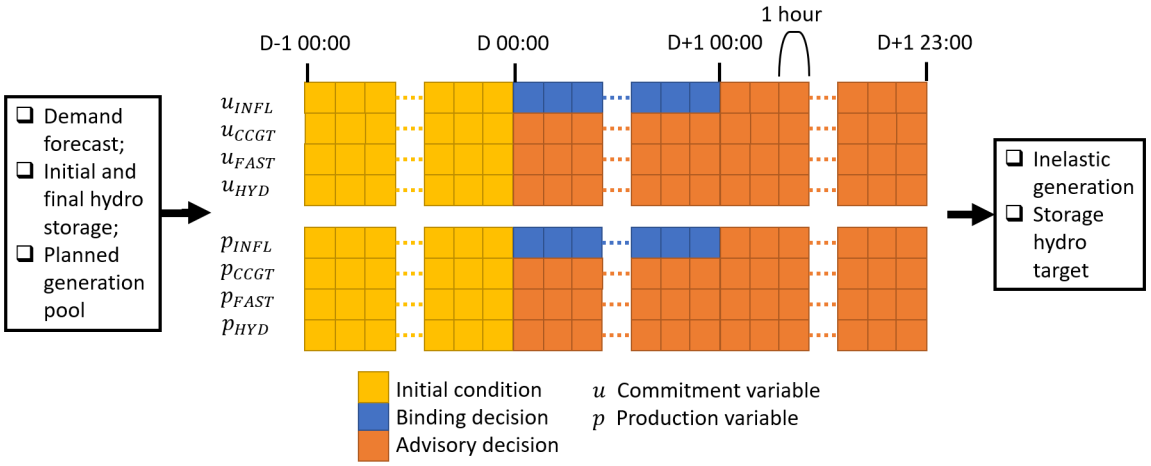

Figure 5: DA UC overview.

launched every 15 minutes over a 1-hour scheduling window.

- **The real-time economic dispatch (RT-ED):** This problem dispatches the generators that are committed in the previous optimization problems.

3.1.1. The Day-Ahead Unit Commitment (DA-UC)

The DA-UC is solved once every day with the goal of serving forecast demand with an hourly granularity. This optimization problem creates two main outputs: (i) the commitment and dispatch of the *inflexible* generators and (ii) a hydro storage target that should be followed by the subsequent real-time optimization problems.

The problem that we solve has a scheduling horizon of 72 hours: (i) 24 hours before the simulated day, (ii) 24 hours for the simulated day and (iii) 24 hours after the simulated day. The first and last 24 hours of the horizon are intended to alleviate boundary conditions. Only the commitment and dispatch of inelastic generators are a binding result of the DA-UC. All other variables are either initial conditions or advisory conditions for subsequent models, as shown in figure 5.

The day-ahead unit commitment is not solved with an ORDC, but by setting reserve requirements that match the historical available balancing capacity in the market. This ensures that our analysis isolates the effect of differences in real-time ORDCs.

3.1.2. The Intermediate Rolling-Window Unit Commitment or Intermediate-RUC

The Intermediate RUC is launched every 6 hours on a 24-hour scheduling window with an hourly granularity. The output of this optimization problem is used to program the commitment of the CCGT units for the next 6 hours, with a 1-hour delay.

Figure 6 provides an overview of an Inter-RUC launched at 5 am. The commitment of the CCGT is fixed during the first period of the scheduling window, and corresponds to the delay that is introduced by the lead-time of the start-up process of CCGT units.

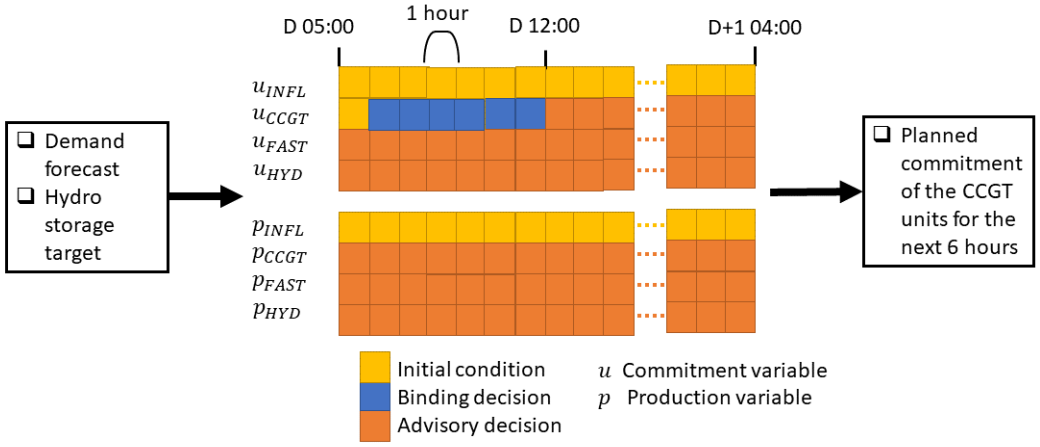

Figure 6: Intermediate-RUC overview.

Only the commitment decision of the CCGT for the next 6 hours will be binding. This includes decisions that are taken in the last binding periods that have repercussions that outlast the binding period. For example, a generator with a 3-hour start-up time and a 2-hour minimum up-time begins its start-up at 10 am. The generator will only be activated at 1 pm and will have to run until 3 pm. The period from 12 pm to 3 pm will also be locked in that situation even though it is not part of the binding period indicated in blue in figure 6.

All the dispatch variables are advisory. The commitment of emergency generators and the mode of pump-hydro are also advisory.

This problem is introduced because CCGT units require a long scheduling window in order to be worth committing, due to their high fixed cost and long start-up time. This process mimicks, to a certain extent, the intraday adjustments that take place in the European intraday market.

3.1.3. The Pre-Real-Time Rolling-Window Unit Commitment or PRT-RUC

The pre-real-time rolling window unit commitment is solved every 15 minutes over w 15-minute periods. It represents the last opportunity for the system operator to activate off-line emergency generation for the next 15 minutes. The commitment and hydro mode decision (pump or produce) for the first 15-minute interval are binding. Every other decision of the model is advisory.

In order to reproduce the European balancing process which uses manual frequency restoration reserves with a full activation time of 15 minutes (slow reserves) and automatic frequency restoration reserves with a full activation time of 7.5 minutes (fast reserves), we proceed as follows. The first period of the PRT is divided into two consecutive 7.5-minute dispatch intervals, even though only one commitment decision is linked to both intervals. This models the tension between activating slow reserves that are

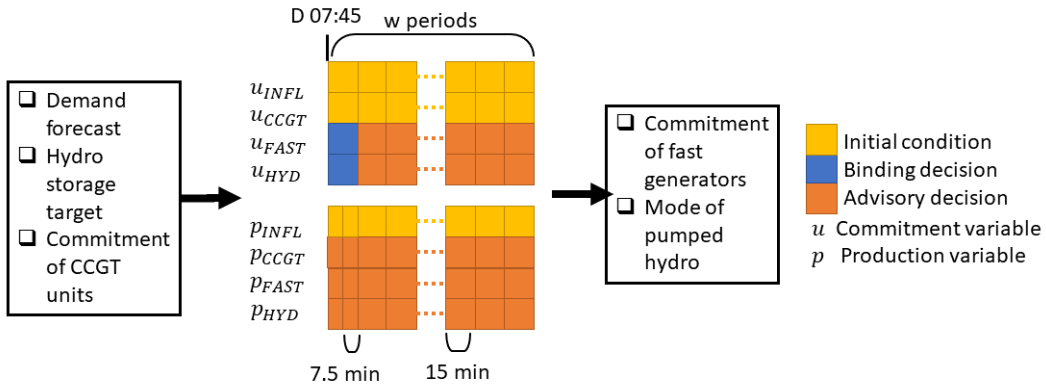

Figure 7: PRT-RUC overview.

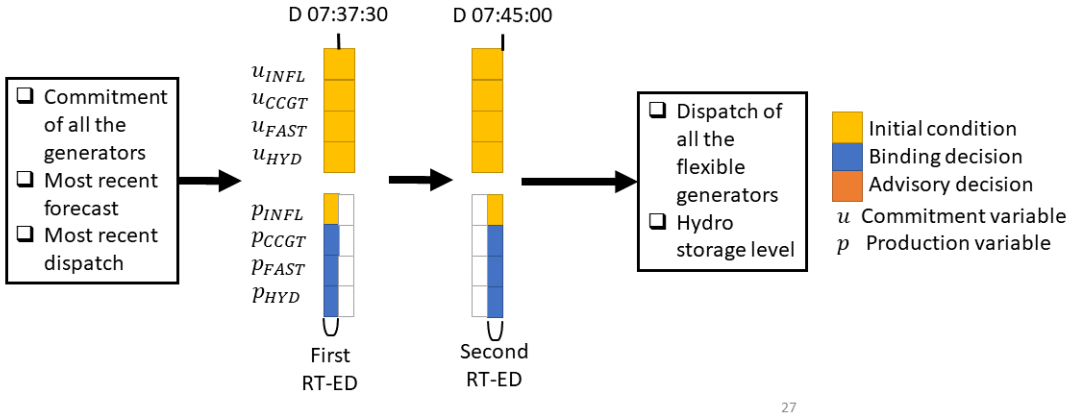

Figure 8: RT-ED overview.

expensive, and using the limited fast reserve available, with the latter option increasing the exposure of the system to imbalances. In our simulation, w is fixed to 4 periods, so that emergency generators are committed with a 1 hour look-ahead.

3.1.4. The Real-Time Economic Dispatch or RT-ED

The real-time economic dispatch model is solved every 7.5 minutes, for a single 7.5-minute period, as indicated in figure 8. Every 15 minutes, the system commits emergency generation and performs two consecutive one-period economic dispatches using the available assets.

3.2. Description of the Full Model

3.2.1. The Day-Ahead Unit Commitment or DA-UC

We define $\mathcal{T} = \{t_1, t_2, \dots t_T\}$ as the scheduling horizon of the DA-UC, D as the day-ahead forecast demand and $\mathcal{S} = \{I, II\}$ as the type of (fast or slow reserve) ORDC considered in this analysis. ORDC I procures reserve resources that can be activated in less than T^I minutes, while ORDC II does the same for resources that can be made available in $T^I + T^{II}$ minutes. Let us also consider $\mathcal{R} = \{MBR_t^i | \forall t \in \mathcal{T}, \forall i \in \mathcal{S}\}$ as the set of segments that define the marginal benefit function of reserve for each period and for each section of that period. We denote as $\mathcal{G} = \{1, 2, \dots N\}$ the set of generators.

The set of decisions concerning a generator g at period t is characterized by the point $x_{g,t} = (p_{g,t}, r^F_{g,t}, r^S_{g,t}, u_{g,t}, v_{g,t}, w_{g,t}, s_{g,t})$. This vector is the concatenation of the production, fast reserve, slow reserve, and binary variables for the commitment, activation, shut-down and start-up of generator g at time t. The vector $x_{g,t}$ belongs to the set $X = \mathbb{R}^3_+ \times \mathbb{B}^4$.

Each generator g is characterized by its cost function $C_g : X \to \mathbb{R}$ and its technical parameters $P^+_g, P^-_g, R_g, UT_g, DT_g$ and SU_g which are respectively the maximum and minimum production limit, the ramp rate, the minimum up time and down time and the start-up time of the unit.

We represent demand for energy and reserve using the vector $m_t = (z_t, r^{T,I}_t, r^{T,II}_t)$. This tuple consists of the shortage in energy and the system supply for reserve for both sections I and II for the period t. The hydro vector $h_t = (p^H_t, d^H_t, e^H_t, r^{H,F}_t, r^{H,S}_t, u^H_t)$ represents the production, consumption, energy stored, fast and slow reserve supplied by pumped hydro, and the pumping mode of a pumped hydro unit for period t. Note that $m_t \in \mathbb{R}^3_+$ and $h_t \in \mathbb{R}^5_+ \times \mathbb{B}^1$.

We further introduce the notation t_- to characterize the period just before t and $t_i : t_j$ as the set of time periods that includes all the periods between t_i and t_j.

We can now fully describe the day-ahead unit commitment problem as follows:

$$P^{DA-UC}(D, \mathcal{T}, \mathcal{R}, \mathcal{G}) = \min_{x_{g,t}, m_t, h_t} \sum_{t \in \mathcal{T}} \Big(\sum_{g \in \mathcal{G}} C_g(x_{g,t}) - \int_0^{r^{T,II}_t} MBR^{II}_t(r) dr - \int_0^{r^{T,I}_t} MBR^{I}_t(r) dr + Voll \cdot z_t \Big) \tag{7a}$$

$$
\begin{aligned}
(s.t.) \quad & D_t = \sum_{g \in \mathcal{G}} p_{g,t} + p_t^H - d_t^H + z_t && \forall t \in \mathcal{T} && \text{(7b)}\\
& r_t^{T,I} \leq \sum_{g \in \mathcal{G}_D} r_{g,t}^F + r_t^{H,F} && \forall t \in \mathcal{T} && \text{(7c)}\\
& r_t^{T,II} \leq \sum_{g \in \mathcal{G}_D} r_{g,t}^S + r_t^{H,S} + r_t^{T,I} && \forall t \in \mathcal{T} && \text{(7d)}\\
& x_{g,t} \in \mathcal{GC}_g && \forall g \in \mathcal{G}, \forall t \in \mathcal{T} && \text{(7e)}\\
& x_{g,t} \in \mathcal{TC}_g^H(x_{g,t_-}) && \forall g \in \mathcal{G}, \forall t \in \mathcal{T} \setminus \{t_0\} && \text{(7f)}\\
& x_{g,t} \in \mathcal{OC}_g^H(x_{g,t_0:t_-}) && \forall g \in \mathcal{G}, \forall t \in \mathcal{T} \setminus \{t_0\} && \text{(7g)}\\
& h_t \in \mathcal{GH} && \forall t \in \mathcal{T} && \text{(7h)}\\
& h_t \in \mathcal{TH}^H(h_{t_-}) && \forall t \in \mathcal{T} \setminus \{t_0\} && \text{(7i)}
\end{aligned}
$$

As stated in the objective (7a), we aim at minimizing the total cost of the system, which is the sum of the production cost and shortage cost minus the marginal benefit from reserve. Shortage is valued at the value of lost load. Equations (7b), (7c) and (7d) are the market clearing constraints for energy, fast and slow reserve. Additionally, the position of every generator at every period needs to respect the generation constraints $\mathcal{GC}_g$, the transition constraints $\mathcal{TC}_g(x_{g,t_-})$ and the operating constraints defined by the space $\mathcal{OC}_g^H(x_{g,t_0:t_-})$, as indicated in equations (7e) to (7g). The same type of constraints applies to pumped hydro, with the pumped-hydro generation constraints $\mathcal{GH}$ and the pumped-hydro transition constraints $\mathcal{TH}^H$ being indicated in equations (7h) and (7i).

The set of constraints for a generator g at time t is then characterized as follows: (8a) and (8c).

$$
\begin{aligned}
\mathcal{GC}_g &= \{x_{g,t} \text{ satisfies (9a)-(9f) }\} && \text{(8a)}\\
\mathcal{TC}_g^H(x_{g,t_-}) &= \{x_{g,t} \text{ satisfies (10a)-(10b) given } x_{g,t_-}\} && \text{(8b)}\\
\mathcal{OC}_g^H(x_{g,t_0:t_-}) &= \{x_{g,t} \text{ satisfies (11a)-(11c) given } \{x_{g,t_0}, \dots x_{g,t_-}\}\} && \text{(8c)}
\end{aligned}
$$

$$
\begin{aligned}
& r_{g,t}^F \leq R_g \cdot T^I && \text{(9a)}\\
& r_{g,t}^S \leq R_g \cdot T^{II} && \text{(9b)}\\
& p_{g,t} + r_{g,t}^F + r_{g,t}^S \leq P_g^+ \cdot u_{g,t} && \text{(9c)}\\
& p_{g,t} \geq P_g^- \cdot u_{g,t} && \text{(9d)}\\
& (p_{g,t}, r_{g,t}^F, r_{g,t}^S) \in \mathbb{R}_+^3 && \text{(9e)}\\
& (u_{g,t}, v_{g,t}, w_{g,t}, s_{g,t}) \in \mathbb{B}^4 && \text{(9f)}
\end{aligned}
$$

Equations (9a) to (9f) represent the ramp constraints on fast and slow reserve, the maximum and minimum technical production limit of a unit, and the definition of the

type of variables (continuous, binary, non-negative, etc.).

$$p_{g,t} - p_{g,t\_} \leq R_g \cdot T^H \cdot (1 - v_{g,t}) + P_g^- \cdot v_{g,t} \tag{10a}$$
$$v_{g,t} + u_{g,t\_} - u_{g,t} - w_{g,t} = 0 \tag{10b}$$

The transition constraints (10a) and (10b) represent the ramp constraint for production and the commitment transition constraint. The production ramp constraint has two possible modes: one for normal operation and one for activation.

$$w_{g,t} + \sum_{t'=max(t_0,t-UT_g^H+1)}^{t} v_{g,t'} \leq 1 \tag{11a}$$
$$v_{g,t} + \sum_{t'=max(t_0,t-DT_g^H+1)}^{t} w_{g,t'} \leq 1 \tag{11b}$$
$$SU_g^H \cdot v_{g,t} - \sum_{t'=max(t_0,t-SU_g^H+1)}^{t-1} s_{g,t'} \leq 0 \tag{11c}$$

The pumped-hydro feasible sets $\mathcal{GH}$ and $\mathcal{OH}^H(h_{t\_})$ at period t can be characterized by equations (12a) and (12b).

$$\mathcal{GH} = \{h_t \text{ satisfies (13a)-(13f)}\} \tag{12a}$$
$$\mathcal{TH}^H(h_{t\_}) = \{h_t \text{ satisfies (13g) given } h_{t\_}\} \tag{12b}$$

$$d_t^H \leq D_H^{Max} \cdot u_t^H \tag{13a}$$
$$e_t^H \leq E_H^{Max} \tag{13b}$$
$$p_t^H + r_t^{H,F} + r_t^{H,S} \leq P_H^{Max} \cdot (1 - u_t^H) \tag{13c}$$
$$p_t^H + r_t^{H,F} + r_t^{H,S} \leq e_t^H \tag{13d}$$
$$(p_t^H, d_t^H, e_t^H, r_t^{H,F}, r_t^{H,S}) \in \mathbb{R}_+^5 \tag{13e}$$
$$u_t^H \in \mathbb{B}^1 \tag{13f}$$
$$e_t^H = e_{t\_}^H - p_{t\_}^H + d_{t\_}^H \cdot \eta \tag{13g}$$

The pumped hydro generation constraints restrict the maximum hydro consumption, energy stored and hydro production in constraints (13a) to (13c) with the pump hydro characteristics D_H^{Max}, E_H^{Max} and P_H^{Max}. Note that the generator is either pumping and

producing as a function of the pumping mode u_t^H. Equation (13d) restricts the hydro reserve to the total stored energy. Constraint (13g) describes the evolution of energy stored in the reservoir as a function of previous period pumping and production decisions, as well as the efficiency of the plant.

The input for $\mathcal{P}^{DA-UC}(D, \mathcal{T}, \mathcal{R}, \mathcal{G})$ is defined as follows:

- $\mathcal{T}$: The set of 72 one-hour periods covering the day before the day of interest, the day of interest and the day after the day of interest.
- D: The day-ahead forecast demand for the net load that needs to be served for each period of $\mathcal{T}$. We provide additional information about the load in section 4.2.
- $\mathcal{R}$: The set of marginal benefit functions for each of the 72 one-hour periods, which are inelastic fixed reserve requirements for the day-ahead unit commitment model. These functions are designed to replicate the historical day-ahead dispatch and as such are not based on a loss of load probability but on the historical reserve available in the system.
- $\mathcal{G}$: The generation pool of controllable assets, which is described in section 4.1.

3.2.2. The Intermediate Rolling-Window Unit Commitment or Inter-RUC

The intermediate rolling window unit commitment requires the solution of the day-ahead unit commitment $\mathbf{X^{DA}}$ defined in (14) to dispatch and commit the inflexible generators belonging to the set $\mathcal{G}_I$, as well as to guide the hydro production and consumption over the day. It is the concatenation of the day-ahead's optimal solution for the generators' variables ($x^{DA,*}$), market variable ($m^{DA,*}$) and the hydro's variable ($h^{DA,*}$). The remaining generators are considered to be dispatchable, and belong to the set $\mathcal{G}_D$.

$$\mathbf{X^{DA}} = (x^{DA,*}, m^{DA,*}, h^{DA,*}) = \arg\max P^{DA-UC} \tag{14}$$

We also introduce the set $\mathbf{X^0}$ that describes the state of the system at the beginning of the scheduling window $\mathcal{T}$. This set includes the dispatch and commitment decisions of the dispatchable generators (x^0), and the level of hydro storage (h^0). This allows us to respect the transition constraints at the beginning of the scheduling window.

In order to describe the commitment constraints of the dispatchable generators in the Inter-RUC problem, we define the concept of the *status* of a generator. This status represents the persisting effect of a decision that may last over the scheduling window of several optimization problems. Every generator g at every period t can belong to one of the 4 following sets, depending on its commitment status:

- $g \in \mathcal{S}_{A,t}$ if the generator g is required to be committed in period t because of an activation decision that occurs in a previous optimization problem and because the minimum up-time constraint of the unit is still active.
- $g \in \mathcal{S}_{U,t}$ if the generator g is required to be down in period t because of a shut-down decision that occurs in a previous optimization problem and because the minimum down-time constraint is still active.

- $g \in \mathcal{S}_{S,t}$ if the generator g is required to be in start-up mode in period t because of an activation decision that occurs in a previous optimization problem.
- $g \in \mathcal{S}_{F,t}$ if the generator g is free to be activated or shut down in period t.

For any period t, a dispatchable generator $g \in \mathcal{G}_D$ must only belong to one status set. In other words, $\cup_{s\in\{A,U,S,F\}}\mathcal{S}_{s,t} = \mathcal{G}_D$ and $\mathcal{S}_{i,t} \cap \mathcal{S}_{j,t} = \emptyset$ for all i and $j \in \{A, U, S, F\}$ with $i \neq j$.

The intermediate rolling window unit commitment problem can now be described as follows:

$$P^{Inter-RUC}(D, \mathcal{T}, \mathcal{R}, \mathcal{G}, \mathcal{S}, \mathbf{X^{DA,*}}, \mathbf{X^0}) =$$

$$\min_{x_{g,t}, m_t, h_t, q_t} \sum_{t\in\mathcal{T}} \Big(\sum_{g\in\mathcal{G}} C_g(x_{g,t}) - \int_0^{r_t^{T,II}} MBR_t^{II}(r)dr - \int_0^{r_t^{T,I}} MBR_t^{I}(r)dr + Voll \cdot z_t + \int_0^{q_t} HD(q)dq \Big) \tag{15a}$$

$$(s.t.) \quad D_t = \sum_{g\in\mathcal{G}} p_{g,t} + p_t^H - d_t^H + z_t \qquad \forall t \in \mathcal{T} \tag{15b}$$

$$r_t^{T,I} \leq \sum_{g\in\mathcal{G}_D} r_{g,t}^F + r_t^{H,F} \qquad \forall t \in \mathcal{T} \tag{15c}$$

$$r_t^{T,II} \leq \sum_{g\in\mathcal{G}_D} r_{g,t}^S + r_t^{H,S} + r_t^{T,I} \qquad \forall t \in \mathcal{T} \tag{15d}$$

$$x_{g,t} \in \mathcal{DAC}(x_{g,t}^{DA,*}) \qquad \forall g \in \mathcal{G}_I, \forall t \in \mathcal{T} \tag{15e}$$

$$x_{g,t} \in \mathcal{GC}_g \qquad \forall g \in \mathcal{G}, \forall t \in \mathcal{T} \tag{15f}$$

$$x_{g,t} \in \mathcal{TC}_g^H(x_{g,t_-}) \qquad \forall g \in \mathcal{G}_D, \forall t \in \mathcal{T} \setminus \{t_0\} \tag{15g}$$

$$x_{g,t_0} \in \mathcal{TC}_g^H(x_g^0) \qquad \forall g \in \mathcal{G}_D \tag{15h}$$

$$x_{g,t} \in \mathcal{OC}_g^H(x_{g,t_0:t_-}) \qquad \forall g \in \mathcal{S}_{t,F}, \forall t \in \mathcal{T} \setminus \{t_0\} \tag{15i}$$

$$x \in \mathcal{SC}(\mathcal{S}) \tag{15j}$$

$$h_t \in \mathcal{GH} \qquad \forall t \in \mathcal{T} \tag{15k}$$

$$h_t \in \mathcal{OH}^H(h_{t_-}) \qquad \forall t \in \mathcal{T} \setminus \{t_0\} \tag{15l}$$

$$h_{t_0} \in \mathcal{OH}^H(h^0) \tag{15m}$$

$$q_t \in \mathcal{DH}(h_t^{DA,*}, h_t) \qquad \forall t \in \mathcal{T} \tag{15n}$$

Compared to the DA-UC problem, a penalty term $\int_0^{q_t} HD(q)dq$ is added to the objective function (15a). It penalizes deviations q_t^H of the real-time hydro storage e_t^H from its day-ahead target level e_t^{DA}. We note that generation constraint (15f), transition constraint (15i), pumped-hydro generating constraint (15k) and pumped-hydro transition constraint (15l) are analogous to the constraints that have already been presented for

the day-ahead problem. Note that the constraints (15h) and (15m) are the transition constraints applied to an initial position. Similarly, the generation operating constraint $\mathcal{OC}_g^H(x_{g,t_0:t_-})$ (15i) only differs from the corresponding day-ahead constraint by being applied only to the free generators. The only new constraints are the day-ahead constraint $\mathcal{DAC}$ (15e), the status constraint $\mathcal{SC}$ (15j) and the hydro deviation constraint $\mathcal{DH}$ (15n), which are defined as follows:

$$\mathcal{DAC}_{g,t}(x_{g,t}^{DA}) = \{x_{g,t} \text{ satisfies (17a)-(17c) given } x_{g,t}^{DA}\} \tag{16a}$$
$$\mathcal{SC}(\mathcal{S}) = \{x \text{ satisfies (18a)-(18c) given } \mathcal{S}\} \tag{16b}$$
$$\mathcal{DH}(h_t^{DA}, h_t) = \{q_t \text{ satisfies (19a)-(19c) given } \{h_t^{DA}, h_t\}\} \tag{16c}$$

$$r_{g,t}^F = 0 \tag{17a}$$
$$r_{g,t}^S = 0 \tag{17b}$$
$$p_{g,t} = p_{g,t}^{DA,*} \tag{17c}$$

The day-ahead constraint captures the inability of inflexible generators to respond to real-time conditions. It restricts the ability of inflexible units to supply reserve (equations (17a) and (17b)). It also does not allow for deviation from the day-ahead dispatch (equation (17c)).

The second group of new constraints concerns the inertia of the commitment decisions:

$$u_{g,t} = 0 \qquad \forall t \in \mathcal{T}, \forall g \in \mathcal{S}_{U,t} \cup \mathcal{S}_{S,t} \tag{18a}$$
$$u_{g,t} = 1 \qquad \forall t \in \mathcal{T}, \forall g \in \mathcal{S}_{A,t} \tag{18b}$$
$$s_{g,t} = 1 \qquad \forall t \in \mathcal{T}, \forall g \in \mathcal{S}_{S,t} \tag{18c}$$

Constraints (18a) and (18b) imply that the generator is either off or on because of the commitment decision of previous problems and their minimum down time and minimum up time constraints. Similarly, (18c) enforces the start-up variables caused by a start-up decision in a previous problem and its start-up time[3]

Finally, $\mathcal{DH}$ describes the feasible set for hydro units: (19a) to (19c).

$$q_t \geq e_t^{DA,*} - e_t^H \tag{19a}$$
$$q_t \geq e_t^H - e_t^{DA,*} \tag{19b}$$
$$q_t \geq 0 \tag{19c}$$

The inputs for the intermediate rolling window unit commitment $P^{Inter-RUC}(D, \mathcal{T}, \mathcal{R}, \mathcal{G}, \mathcal{S}, \mathbf{X^{DA,*}}, \mathbf{X^0})$ launched at time t and following a day-ahead unit commitment $P^{DA}(D^{DA}, \mathcal{T}^{DA}, \mathcal{R}^{DA}, \mathcal{G}^{DA})$ are described as follows.

[3]Note that, although we do not assume a startup profile as in Simoglou [SBB10], we do introduce a delay between the moment we decide to start up a unit and the moment that the unit is actually online. This has a significant impact on the interplay between the choice of ORDC and security, as we discuss in section 4.

- $\mathcal{T}$: A 24 one-hour period subset of $\mathcal{T}^{DA}$ covering the 24 hours following time t (the launch of the problem). This set corresponds to a one-day scheduling window that evolves as the day progresses.
- D: The most recent demand forecast available at time t for each period of $\mathcal{T}$.
- $\mathcal{R}$: The set of marginal benefit functions for each of the 24 one-hour periods. The marginal benefit functions are driven by (i) the mean and standard deviation of the system imbalance, which are dependent on the time of the day and the season, and (ii) the variant of ORDC analysed. The estimation of the parameters of the system imbalance is discussed in section 4.3. More information on the ORDC variants can be found in section 2.3.
- $\mathcal{G}$: The generation pool of controllable assets is defined in section 4.1. This pool can differ from $\mathcal{G}^{DA}$, depending on random outages that may occur in the system.
- $\mathcal{S}$: The partition of generators by status, depending on their availability. This set evolves according to the decision of the intermediate rolling window unit commitment problem solved before time t. Section 3.2.5 describes the rules that are used for constructing this set. Note that $\mathcal{S}_{t_0,F}$ is empty.
- $\mathbf{X^{DA,*}}$: The set of solutions of the day-ahead unit commitment as characterized by (14).
- $\mathbf{X^0}$: The set describing the state of the system in t_-. This set includes the dispatch and commitment position and the hydro storage level in t_-.

3.2.3. The Pre-Real-Time Rolling-Window Unit Commitment or PRT-RUC

The scheduling window for the pre-real time problem is defined as $\mathcal{T} = \{t_{0,0}, t_{0,1}, t_1, \ldots, t_{w-1}\}$. It represents two 7.5-minute periods ($t_{0,0}$ and $t_{0,1}$) and $w-1$ 15-minute periods. This window plans over $w \cdots 15$ minutes. The first period is split, in order to account for the start-up profile of emergency generators and how much of their generation is available after 7.5 minutes. The problem can be formulated as follows:

$$P^{PRT-RUC}(D, \mathcal{T}, \mathcal{R}, \mathcal{G}, \mathcal{S}, \mathbf{X^{DA,*}}, \mathbf{X^0}) =$$

$$\min_{x_{g,t}, m_t, h_t, q_t} \frac{1}{8} \sum_{t \in \{t_{0,0}, t_{0,1}\}} \Big(\sum_{g \in \mathcal{G}} C_g(x_{g,t}) - \int_0^{r_t^{T,II}} MBR_t^{II}(r)dr - \int_0^{r_t^{T,I}} MBR_t^{I}(r)dr + Voll \cdot z_t + \int_0^{q_t} HD(q)dq \Big)$$

$$+ \frac{1}{4} \sum_{t \in \mathcal{T} \setminus \{t_{0,0}, t_{0,1}\}} \Big(\sum_{g \in \mathcal{G}} C_g(x_{g,t}) - \int_0^{r_t^{T,II}} MBR_t^{II}(r)dr - \int_0^{r_t^{T,I}} MBR_t^{I}(r)dr + Voll \cdot z_t + \int_0^{q_t} HD(q)dq \Big) \tag{20a}$$

$$
\begin{aligned}
(s.t.) \quad & D_t = \sum_{g \in \mathcal{G}} p_{g,t} + p_t^H - d_t^H + z_t && \forall t \in \mathcal{T} && \text{(20b)}\\
& r_t^{T,I} \leq \sum_{g \in \mathcal{G}_D} r_{g,t}^F + r_t^{H,F} && \forall t \in \mathcal{T} && \text{(20c)}\\
& r_t^{T,II} \leq \sum_{g \in \mathcal{G}_D} r_{g,t}^S + r_t^{H,S} + r_t^{T,I} && \forall t \in \mathcal{T} && \text{(20d)}\\
& x_{g,t} \in \mathcal{DAC}(x_{g,t}^{DA,*}) && \forall g \in \mathcal{G}_I, \forall t \in \mathcal{T} && \text{(20e)}\\
& x_{g,t} \in \mathcal{GC}_g && \forall g \in \mathcal{G}, \forall t \in \mathcal{T} && \text{(20f)}\\
& x_{g,t} \in \mathcal{TC}_g^{15}(x_{g,t_-}) && \forall g \in \mathcal{G}_D, \forall t \in \mathcal{T} \setminus \{t_{0,0}, t_{0,1}\} && \text{(20g)}\\
& x_{g,t} \in \mathcal{OC}_g^{15}(x_{g,t_0:t_-}) && \forall g \in \mathcal{S}_{t,F}, \forall t \in \mathcal{T} \setminus \{t_0\} && \text{(20h)}\\
& x_{g,t_{0,0}:t_{0,1}} \in \mathcal{SUC}g(x_g^0) && \forall g \in \mathcal{G}_D && \text{(20i)}\\
& x \in \mathcal{SC}(\mathcal{S}) && && \text{(20j)}\\
& h_t \in \mathcal{GH} && \forall t \in \mathcal{T} && \text{(20k)}\\
& h_t \in \mathcal{TH}^{15}(h_{t_-}) && \forall t \in \mathcal{T} \setminus \{t_0\} && \text{(20l)}\\
& h_{t_{0,0}} \in \mathcal{TH}^{7.5}(h^0) && && \text{(20m)}\\
& h_{t_{0,1}} \in \mathcal{TH}^{7.5}(h_{t_{0,0}}) && && \text{(20n)}\\
& q_t \in \mathcal{DH}(h_t^{DA}, h_t) && \forall t \in \mathcal{T} && \text{(20o)}
\end{aligned}
$$

The PRT-RUC resembles the intermediate-RUC, with the main difference being in the temporal granularity. The difference in time granularity requires adjustments in: the objective function (20a); the transition and operating constraints $\mathcal{TC}^{15}$ and $\mathcal{OC}^{15}$: the newly introduced start-up constraint $\mathcal{SUC}$ that defines the start-up profile of the generators; and the hydro transition constraints $\mathcal{TH}^{15}$ and $\mathcal{TH}^{7.5}$.

The granularity in this model is 7.5 minutes for the first 15 minutes and then 15 minutes for the next $(w-1)\cdots 15$ minutes. This allows us to account for the start-up profile of the emergency generators. This is expressed in the following startup constraints:

$$
\mathcal{SUC}_{g,t}(x_g^0) = \{\{x_{g,t_{0,0}}, x_{g,t_{0,1}}\} \text{ satisfies (22a)-(22e) given } x_g^0\} \tag{21}
$$

$$
\begin{aligned}
& p_{g,t_{0,0}} - p_g^0 \leq R_g \cdot T^{7.5} \cdot (1 - v_{g,t}) + R_g^{SU,0} \cdot v_{g,t} && \text{(22a)}\\
& p_{g,t_{0,1}} - p_{g,0,1} \leq R_g \cdot T^{7.5} \cdot (1 - v_{g,t}) + R_g^{SU,1} \cdot v_{g,t} && \text{(22b)}\\
& v_{g,t_{0,1}} + u_g^0 - u_{g,t_{0,1}} - w_{g,t_{0,1}} = 0 && \text{(22c)}\\
& u_{g,t_{0,0}} = u_{g,t_{0,1}} && \text{(22d)}\\
& v_{g,t_{0,0}} = v_{g,t_{0,1}} && \text{(22e)}
\end{aligned}
$$

The startup constraints (22a) and (22b) ensure that generators comply with their start-up profile. This startup profile is characterized by their maximum production 7.5

minutes and 15 minutes after activation ($R_g^{SU,0}$ and $R_g^{SU,1}$). Note that the two 7.5-minute dispatch periods only account for one 15-minute commitment period.

The 7.5 and 15-minute hydro transition constraints are described as follows:

$$e_t^H = e_{t_-}^H - \frac{1}{8} \cdot (p_{t_-}^H + d_{t_-}^H \cdot \eta) \tag{23a}$$

$$e_t^H = e_{t_-}^H - \frac{1}{4} \cdot (p_{t_-}^H + d_{t_-}^H \cdot \eta) \tag{23b}$$

The inputs for the pre-real-time rolling-window unit commitment are similar to the ones used in the intermediate rolling-window unit commitment. The one difference is the set of periods, which now includes two 7.5-minute periods at the beginning of the optimization horizon.

3.2.4. The Real-Time Economic Dispatch or RT-ED

The economic dispatch model does the best it can with what was committed in the previous commitment model. It is a one period economic dispatch that can be described as follows:

$$P^{RT-ED}(D, \mathcal{R}, \mathcal{G}, \mathcal{S}, \mathbf{X^{DA,*}}, \mathbf{X^0}) =$$

$$\min_{x_g, m, h, q} \frac{1}{8}\Big(\sum_{g \in \mathcal{G}} C_g(x_g) - \int_0^{r^{T,II}} MBR^{II}(r)dr - \int_0^{r^{T,I}} MBR^{I}(r)dr + Voll \cdot z + \int_0^{q} HD(q')dq' \Big) \tag{24a}$$

$$(s.t.) \quad D = \sum_{g \in \mathcal{G}} p_g + p^H - d^H + z \tag{24b}$$

$$r^{T,I} \leq \sum_{g \in \mathcal{G}_D} r_g^F + r^{H,F} \tag{24c}$$

$$r^{T,II} \leq \sum_{g \in \mathcal{G}_D} r_g^S + r^{H,S} + r^{T,I} \tag{24d}$$

$$x_g \in \mathcal{DAC}(x_g^{DA,*}) \qquad \forall g \in \mathcal{G}_I \tag{24e}$$

$$x_g \in \mathcal{GC}_g \qquad \forall g \in \mathcal{G} \tag{24f}$$

$$x_g \in \mathcal{TC}_g^{7.5}(x_g^0) \qquad \forall g \in \mathcal{G}_D \tag{24g}$$

$$x \in \mathcal{SC}(\mathcal{S}) \tag{24h}$$

$$h \in \mathcal{GH} \tag{24i}$$

$$h \in \mathcal{TH}^{7.5}(h^0) \tag{24j}$$

$$q \in \mathcal{DH}(h^{DA,*}, h) \tag{24k}$$

The RT-ED problem is is similar to the first period of the PRT-RUC except for the status constraint (24h). None of the generator is free and $\mathcal{S}_U \cup \mathcal{S}_A \cup \mathcal{S}_S = \mathcal{G}_D$. The commitment of the generators are fixed by that constraint.

3.2.5. Updating the Collection of Status Set, $\mathcal{S}$

At the end of every intermediate rolling window unit commitment and pre-real-time rolling-window unit commitment, the collection of status set needs to be updated. At every period t, the set $\mathcal{S}$ is updated as follows:

1. If the generator g is activated in time t, then g is moved to the start-up generators from t to $t + SU_g$ and to the activated generators from $t + SU_g$ to $t + SU_g + UT_g$.

2. If the generator g is shut down in time t, then g is moved to the unavailable generators from t to $t + DT_g$.

It is also possible that a generator unavailable because of the minimum down time constraint begins its startup process to be commited after the minimum down is over. In this situation, g will be moved in the startup generator set from t to $t + SU_g$ and to the activated generator set from $t + SU_g$ to $t + UT_g$.

Once the effect on an activation or a shutdown decision is no longer binding, a generator is moved again to the set of free generators.

4. Populating the Model with Data

4.1. Generation Pool

The generation pool modelled in the simulator includes all the controllable assets of Belgium and is mainly based on the database of installed capacity by unit, which is publicly available on the Elia website [ELI]. This generation pool is described in table 1, and includes 7500 MW of inflexible generation scheduled in the day ahead, and approximately 4300 MW of flexible generation that can be further subdivided into fast balancing capacity and slow balancing capacity. In addition, we introduce to the model pumped-hydro capacity, foreign balancing capacity which is also referred to as Inter-TSO capacity and non-CIPU generation. Non-CIPU assets are defined as assets that do not engage in the standard contract for the Coordination of the Injection of Production Units (CIPU), but can nevertheless participate in the balancing market.

Type of Dispatch and commitment		Type of plant	Number of units	Maximum aggregated production [MW]	Ability to provide reserve
Inelastic		Cogeneration units Run of river hydro Waste incinerators Nuclear Classical		7 500	No
Flexible	Fast balancing capacity	CCGT	8	3 230	Yes
		CCGT-CHP	2	524	Yes
		OCGT	6	302	Yes
	Slow balancing capacity	Turbo-jet	10	194	Yes
		Non-CIPU		250 to 500	Yes
Pump-Hydro				1 300	Yes
Inter-TSO				50	Yes

Table 1: Generation pool used in our analysis.

4.1.1. Inelastic Units

The inelastic assets are composed of cogeneration units, run of river hydro, waste incinerators, nuclear generation and wood pellet generators (indicated in the table as classical generation). Inelastic units are assumed to follow their historical production, as opposed to following the price signal of a short-term market. This may either be the case because the technology is too slow or costly in terms of adjusting its output, or because its power output is also linked to other economic processes.

	Minimum up time [min]	Minimum down time [min]	Start-up time [min]	Minimum stable power [% PMax]	Ramp rate [%PMax/min]
CCGT	180	180	60	30 to 55	3 to 8
CCGT-CHP	180	180	60	35 to 50	1 to 3
OCGT	160	60	10	20 to 45	15 to 30
Turbo-jet	0	6	3	100	100
Non-CIPU	15	15	15	100	100

Table 2: Technical parameters of flexible assets that relate to the operating constraints of the assets.

D_H^+	P_H^+	E_H^+	η
1195	1213	11280	0.76

Table 3: Parameters of pumped-hydro units.

4.1.2. Flexible Units

The flexible assets include (i) CCGT plants and (ii) CCGT-CHP plants, with the latter being cheaper to run than the former, (iii) OCGT plants that can supply fast balancing capacity when they are online and slow balancing capacity when offline and (iv) turbo-jet, and (v) non-CIPU generation. The last two are assumed to provide slow balancing capacity. CIPU assets are individually modelled and non-CIPU generation is an aggregation of the historical non-CIPU generation from the historical ARC. The technical parameters of these plants can be found in table 2, and are similar to the ones used in [ELI19].

Flexible generators can either be classicals (CCGT, CCGT-CHP and OCGT) or *all-or-nothing* (turbo-jet and non-CIPU). Classicals generators have variable outputs and incurs fixed and activation cost. A complete description of their cost function can be found in appendix B. All or nothing generators have fixed outputs and technology dependent marginal cost. Turbo jet's marginal cost is equal to 315 € per MWh following [PSB17]. Non-CIPU's marginal cost is obtained from the historical data of the merit order curve of the ARC [ELI21] and varies from 270 to 2300 € per MWh. The amount of non-CIPU capacity available in a particular day is given by the historical level of R3 Flex that is selected by ELIA on that day.

4.1.3. Pumped Hydro

The maximum consumption of pumped hydro generation is obtained by adding the consumption from COO I (3 145 MWh pumps), COO II (3 200 MWh pumps) and Plate-Taille (4 40 MWh pumps). The same process is used for estimating the maximum production capacity (3 144 MWh turbines for COO I, 3 215 MWh turbines from COO II and 4 34 MWh turbines for Plate-Taille).

4.1.4. Inter-TSO Capacity

Foreign balancing capacity is modelled as an affine supply function, following [**?**]. The maximum unscheduled import capacity from neighbouring markets is set at 50 MW, following [ELI20].

4.1.5. Mapping Technologies Used in the Model to Technologies Available in the Belgian Databases

The Available Regulation Capacity or ARC is central in Belgium when discussing balancing capacity in general, and scarcity pricing in particular. It represents the expected level of balancing capacity that will be available in Belgium from the day-ahead and intra-day point of view. The ARC is currently used for computing the *scarcity prices-adders* on the ELIA website. In order to understand how the balancing capacity of Belgium is translated in our model, it is important to discuss how this balancing capacity is mapped to the ARC, and what type of balancing capacity is available for serving the demand of each ORDC (the 7.5-minute ORDC and the 15-minute ORDC). This is needed in order to avoid missing or double-counting available balancing resources.

The full balancing capacity is composed of flexible CIPU assets (CCGT, OCGT and turbojet plants), flexible non-CIPU assets (also referred to as non-CIPU balancing capacity), pumped hydro, and foreign balancing capacity. All of these capacities are included in the ARC under one or several of the different categories of balancing capacity as described in figure 9. These categories include reserved balancing capacity (R2 and R3), as well as non-reserved balancing capacity (which consists of CIPU coordinable, CIPU limited coordinable, non-CIPU coordinable and Inter-TSO). Reserved balancing capacity is auctioned in forward reserve markets, whereas non-reserved capacity is only remunerated upon activation. The ARC can also be partitioned in terms of mFRR/aFRR, with R2 being an aFRR product and R3, CIPU coordinable, CIPU limited Coordinable and Non-CIPU coordinable being mFRR products. The details of the mapping are described hereunder and in figure 9:

1. CCGT plants can participate in the R2 and R3 auctions. All non-selected capacity is listed as CIPU coordinable. Only online CCGT units are eligible for reserve, as they have a long start-up time.

2. Online OCGT plants can be selected as R2 and offline OCGT are eligible for the R3 auction. All the non-selected capacity is included as CIPU coordinable.

3. Turbojet plants are usually offline. Therefore, they are not included in R2, but are eligible for R3 auctions and as CIPU coordinable.

4. Pumped hydro participates in R2 auctions. However, its full balancing capacity, which should take into account the level of hydro storage and the availability of the turbine, is not included in the ARC. The accurate representation of the full pumped hydro flexibility requires the introduction of an additional product that is referred to as hydro margin.

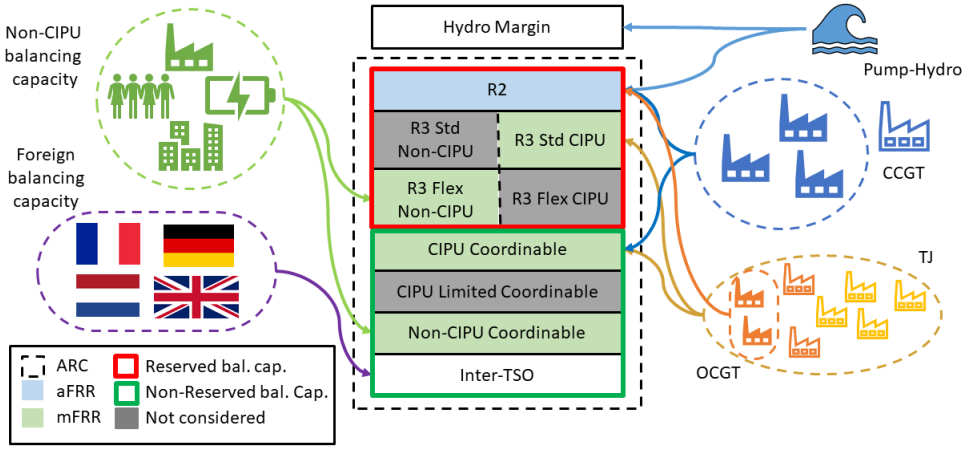

Figure 9: Mapping of the balancing capacity to the ARC.

5. Non-CIPU balancing capacity is eligible for R3 and non-CIPU coordinable.

6. Foreign balancing capacity is included as Inter-TSO.

Note that R3 can be subdivided as a function of the source of the balancing capacity (CIPU or non-CIPU assets) and the quality of the product (Standard or Flex), with CIPU assets participating in the Standard auctions and Non-CIPU assets mostly participating in the Flex auctions. Finally, CIPU limited coordinable represents a small amount of capacity, and is therefore not included in that mapping.

The amount of non-CIPU balancing capacity in a given day is extracted from the ARC. On the other hand, CIPU assets are modelled individually. Modelling these assets therefore does not explicitly require the historical ARC for computing the level of CIPU-based balancing capacity. The simulation differs from the study performed by ELIA [ELI18], which only accounts for the historical level of the ARC when computing the adder.

To conclude the mapping of the balancing capacity, the reactivity of the different types of generators and their availability for serving the demand of the different ORDCs need to be explicitly characterized. This availability represents the generation that can be made available in 7.5 minutes for the 7.5-minute ORDC and in 15 minutes for the 15-minute ORDC.

1. The supply of CCGT plants to the 7.5-minute and 15-minute ORDC is restricted by their ramp rate.

2. Online OCGT plants are restricted by their ramp when serving the 7.5-minute ORDC. Offline OCGT plants can provide their full production to the 15-minute ORDC. A fraction ρ of their total capacity is eligible for contributing to the demand of the 7.5-minute ORDC.

3. Turbojet plants can provide their full capacity within 15 minutes. They can make up to a fraction ρ of their total capacity within 7.5 minutes.

4. Pumped hydro units are eligible for both the 15 and 7.5-minute ORDCs.

5. Non-CIPU generators can provide their full capacity within 15 minutes, and are eligible up to a factor ρ of their nominal capacity for the 7.5-minute ORDC.

6. Foreign balancing capacity is eligible for the 15-minute ORDC. The fraction of that capacity which is eligible for the 7.5-minute ORDC is further analyzed in a sensitivity study in section 6.5.

The factor ρ described above was set at 50% by default in [ELI18]. A sensitivity analysis on that parameter is performed in section 6.4 for values of 0, 28 and 50%.

4.2. Net Load

What we mean by net load is the difference between grid load and renewable energy and imports / exports. In other words, this is the power that must be served by flexible and controllable assets. Figure 10 illustrates the difference between the grid load and the net load during an indicative 4-day period in November 2018.

The data that we use for net load is obtained from ELIA [ELI21] and the ENTSO-E transparency platform [EE21]. The data resolution of the ELIA website and ENTSO-E platform are respectively 15-minute and hourly.

4.3. Imbalance

ELIA records system imbalance at a 15-minute resolution. The data is available in [ELI21]. This imbalance data is used for estimating an ORDC, as discussed in section 3. In particular, we require an estimate of the mean and standard deviation of the distribution of imbalances for every season and for every 4-hour block of the day for which we design an ORDC. In table 8 we present the parameters of the Belgian imbalances that have been used to simulate the year 2018. They have been estimated from the data of 2015 to 2017.

[4]Block 1 is 10 pm to 2 am, block 2 is 2 am to 6 am, block 3 is 6 am to 10 am, block 4 is 10 am to 2 pm, block 5 is 2 pm to 6 pm and block 6 is 6 pm to 10 pm.

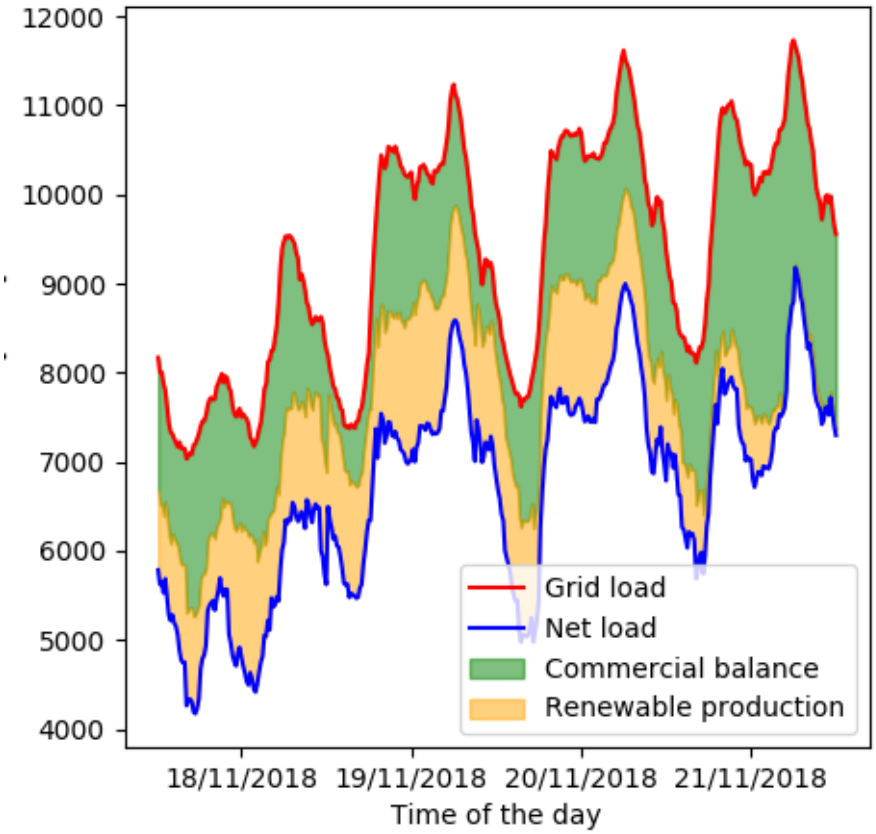

Figure 10: Grid load and net load for November 18th - 21st, 2018.

Season	Time of the day[4]	Mean	Standard deviation
Winter	Block 1	29.00	160.25
Winter	Block 2	25.93	134.12
Winter	Block 3	6.77	165.30
Winter	Block 4	44.00	190.88
Winter	Block 5	56.95	169.15
Winter	Block 6	3.99	144.29
Spring	Block 1	7.74	145.75
Spring	Block 2	27.05	128.75
Spring	Block 3	-0.86	143.95
Spring	Block 4	28.81	173.13
Spring	Block 5	40.64	159.02
Spring	Block 6	-7.44	127.18
Summer	Block 1	14.54	134.15
Summer	Block 2	27.89	111.75
Summer	Block 3	0.86	130.06
Summer	Block 4	28.98	151.59
Summer	Block 5	27.60	144.17
Summer	Block 6	-5.93	119.16
Autumn	Block 1	11.62	151.34
Autumn	Block 2	29.19	124.09
Autumn	Block 3	-21.08	160.09
Autumn	Block 4	-7.58	175.77
Autumn	Block 5	-5.30	144.98
Autumn	Block 6	-10.95	150.09

Table 4: Mean and standard deviation of the 15-minutes imbalance distribution

5. Validation of the market model

In this section we measure the performance of the simulator against the historical realisations of the system. This process is performed by assessing the quality of the forward position computed by the day-ahead unit commitment compared to the historical day-ahead position. The validation is restricted to the day-ahead unit commitment because the co-optimization of reserve and energy in real time in our simulator is a closed-loop investigation that is expected to produce a different dispatch depending on the ORDC that we analyse.

5.1. Day-Ahead Unit Commitment

The most important task of the day-ahead unit commitment is to characterize accurately the energy transfer between natural gas production and pumped hydro, as indicated in figure 11. This graph shows that, during periods of low load, a part of the production is transferred to hydro storage through pumping, so as to be reused later during peak-load periods.

The comparison is performed over the aggregated forecast production per type of fuel. There are five types of fuel, namely (i) nuclear, (ii) other, (iii) gas, (iv) hydro, and (v) liquid fuel. As stated previously, we will mostly focus on gas and hydro production. Nuclear and other technologies are mainly driven by the maximum available output and liquid fuel is used as an emergency measure and is rarely scheduled in the day ahead. Figure 12 presents the usual output of the DA-UC, and compares it to the historical forecast production. Only the center of those graphs (between the dashed red lines) is relevant in our discussion. These outputs exhibit stable production for nuclear and other, no production from liquid fuel, and a varying level for natural gas and hydro.

We can observe the following:

1. Natural gas production is periodic and heavily influenced by the type of day that is simulated, as indicated in Fig. 13. For example, the winter break of 2018 lasted until the 7th of December and this can be seen on the graph with lower production during those periods. As indicated in table 5, the simulator MAE and RMSE for gas production are 208.8 MW and 267.7 MW respectively. In comparison to previous analyses in [PSB17] with an MAE of 240.8 MW and an RMSE of 309.9 MW, we find that our model attains comparable accuracy.

2. Hydro generation is mainly used during peak load periods, as we can observe from the spikes of Fig. 14. The magnitude of the simulated and historical spikes may differ, but the profiles are largely similar. The MAE and RMSE of hydro are 69.2 MW and 113.7 MW, which are comparable to the values of 61.9 MW and 119.3 MW respectively that have been found in [PSB17].

The simulator is an extension of [PSB17]. It improves the previous version by (i) refining and extending the generation pool, (ii) reducing the granularity of the dispatch and (iii) proposing a more realistic modeling of the dispatch and commitment decisions.

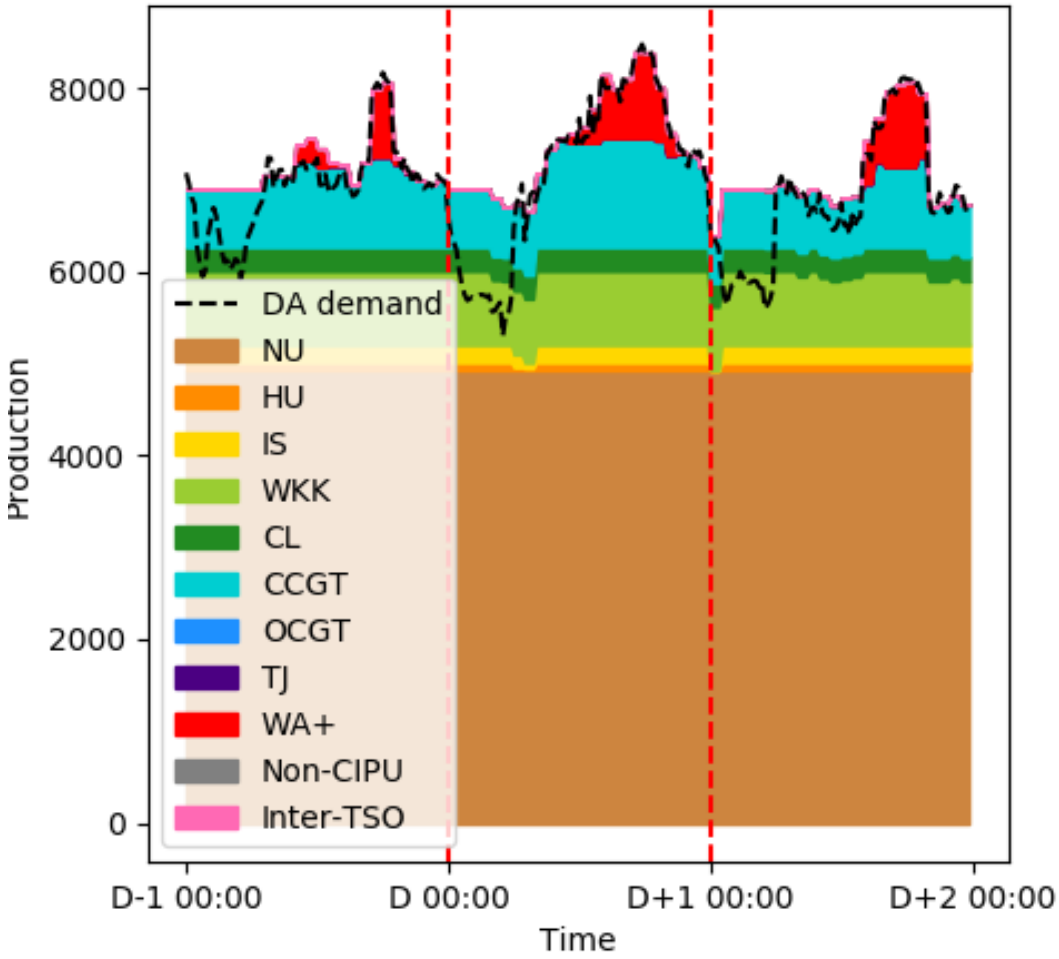

Figure 11: Forecast production of the simulator according to the DA-UC model.

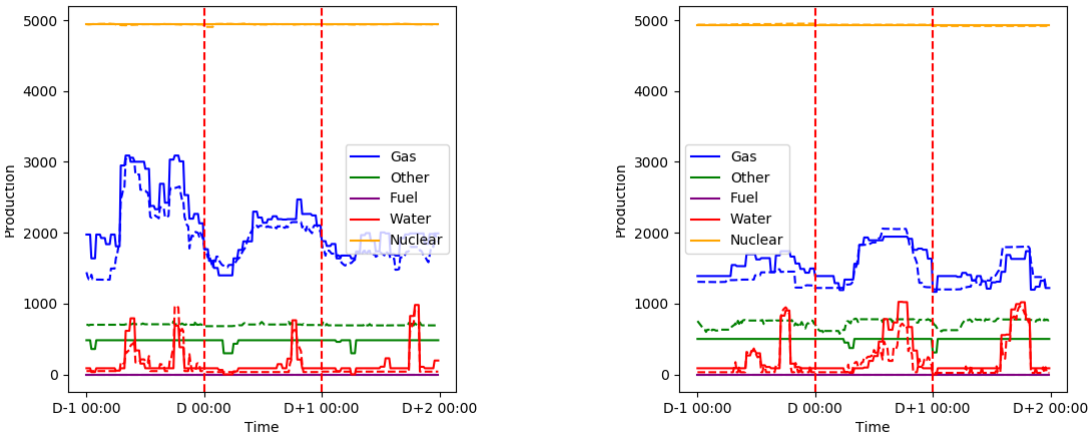

(a) 03/02/2018

(b) 04/01/2018

Figure 12: Comparison of historical (dotted line) and simulated (full line) day-ahead forecast production per type of fuel.

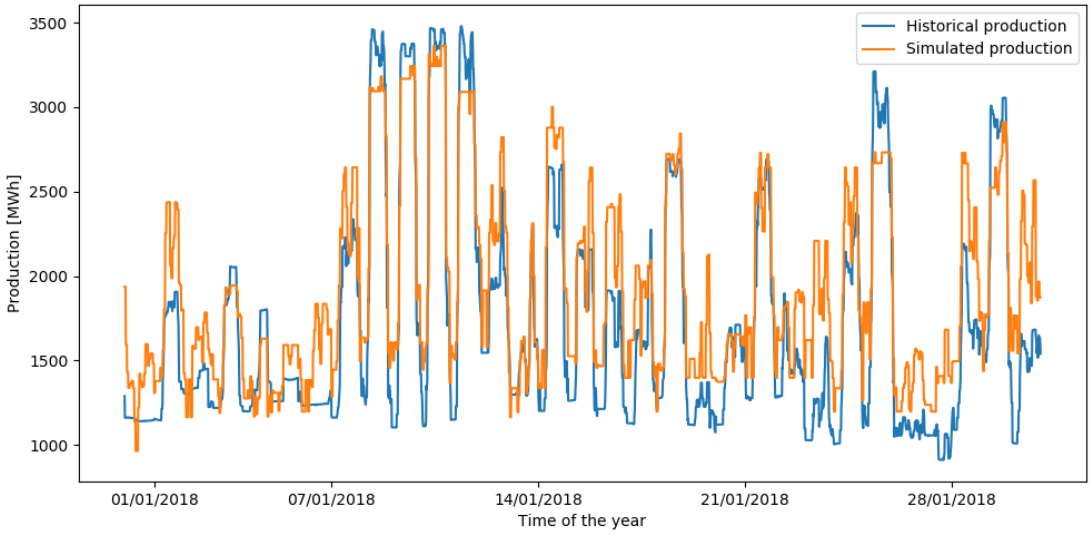

Figure 13: Comparison of historical and simulated day-ahead forecast gas production for January 2018.

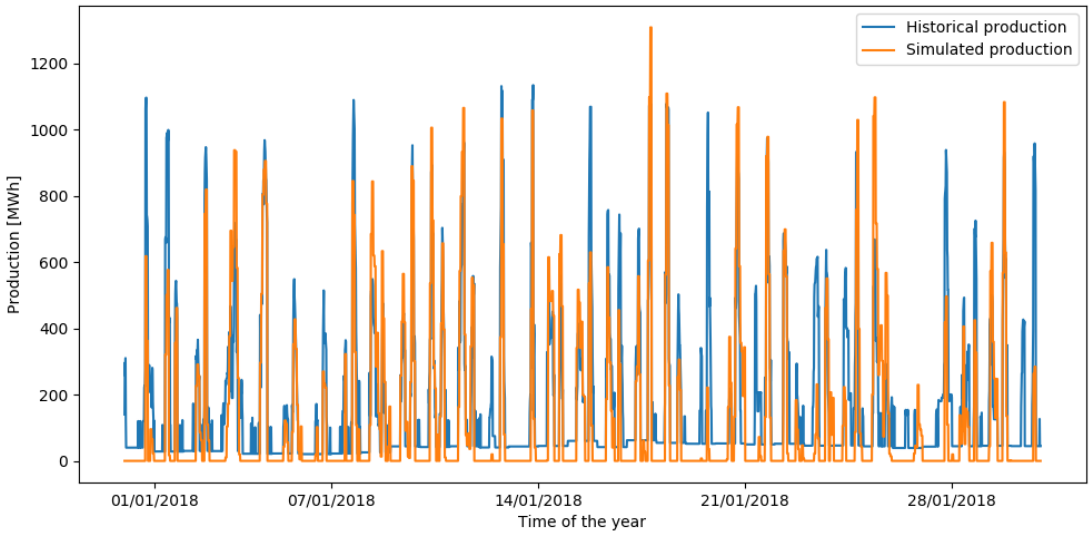

Figure 14: Comparison of historical and simulated day-ahead forecast water production for January 2018.

		Gas	Water	Fuel	Other	Nuclear
ME	Simulator	-76.7	28.5	0.0	140.4	2.7
	1st Study	168.9	4.7			
MAE	Simulator	208.8	69.2	0.0	148.7	36.8
	1st Study	240.7	61.6			
RMSE	Simulator	267.7	113.7	1.0	176.9	116.2
	1st Studay	309.9	119.3			

Table 5: Mean Error (ME), Mean Absolute Error (MAE) and Root Mean Squared Error (RSME) between the historical and simulated production per type of fuel for 2018 and comparison with the errors of the study in [PSB17] for 2013.

These enhancements allow us to analyse the tradeoff between the commitment of fast balancing capacity and the cost of operating the system with more realism. Table 5 compares the simulator with [PSB17] and shows that the increased modeling detail does not come at the cost of accuracy in replicating past observations of the Belgian electricity system.

6. Results

The results presented in this section are obtained by simulating the historical demand of Belgium for 2018. We consider a reference scenario, according to which (i) 25 MW of aFRR will be available at all time from foreign balancing capacity, (ii) 28% of the mFRR balancing capacity that is available in real time will be available for covering the demand of the 7.5-minute ORDC and (iii) 10 MW of aFRR balancing capacity are available from demand response.

In addition to the reference scenario, we perform a sensitivity analysis on a number of parameters that are changed relative to their value in the reference scenario:

1. 0, 25 MW or 50 MW of aFRR can be made available from foreign balancing capacity,
2. 0%, 28% or 50% of mFRR balancing capacity can be used for covering the demand of the 7.5-minute ORDC,
3. 0 MW or 10 additional MW of aFRR capacity can be covered by demand response.

The sensitivity scenarios analysed here can be linked to [ELI18], but differ in terms of accounting for different levels of availability for mFRR balancing capacity. The closest comparison would be the best-case scenario in [ELI18] and the 25 MW of aFRR from foreign balancing capacity and 50% availability of mFRR balancing capacity in our simulator.

Our analysis focuses on comparing the total operating cost of the different variants and on analyzing the impact of these variants on the level of the adder. We additionally quantify a number of additional metrics, including the energy not served and the loss of load probability. The comparison focuses largely on the level of conservatism of the variants. More conservative variants (value of lost load at 13500 €/MWh and / or independent 7.5-minute imbalance increments) will be measured against less conservative variants (value of lost load at 8300 €/MWh and / or correlated 7.5-minute increments).

6.1. Cost Analysis of the Reference scenario

The total cost of the variants is reported in table 6. The values reported here are obtained by adding the fuel cost, fixed cost, activation cost and shortage cost of the system, and do not include the cost of the price-inelastic generators, since the latter is identical across different scenarios. The total cost varies from 1.69 M € per day to 1.68 M € per day. Thus, we find a difference of up to 10 k € per day between the different variants. This corresponds to a variation of up to 0.8% of the mean total flexible cost, which can be considered quite stable. Despite the stability of the total cost, we conduct a detailed analysis of the differences between the variants. This analysis allows us to better understand the impact of the ORDC on the commitment and dispatch decisions.

We can already extract some trends from table 6:

			Total cost M€/Day	Fuel cost	Fixed cost	Activ. cost	Short. cost
8300	Pre-Activation	Independent	1.694	1.317	0.344	0.032	0.001
		Correlated	1.697	1.321	0.342	0.033	0.000
	Post-Activation	Independent	1.691	1.316	0.343	0.032	0.000
		Correlated	1.694	1.318	0.343	0.033	0.000
13500	Pre-Activation	Independent	1.688	1.304	0.352	0.031	0.000
		Correlated	1.687	1.302	0.350	0.033	0.002
	Post-Activation	Independent	1.684	1.301	0.352	0.031	0.000
		Correlated	1.683	1.299	0.350	0.033	0.000

Table 6: Decomposition of the mean total operating cost of each variant in million euros per day.

1. More conservative variants are typically less costly. This trend is more accentuated for the variation of the VOLL, where the 13500 variants are consistently cheaper than their 8300 counterpart.

2. The simulation of the system with the reference generation pool as described in section 4 is not susceptible to load shedding, as indicated by the negligible shortage cost.

3. Both pre- and post-activation variants yield a similar level of cost, with the post-activation variants being slightly cheaper.

4. The fuel cost accounts for 77.16 to 77.85% of the total cost, the fixed cost for 20.17 to 20.92%, the activation cost for 1.85 to 1.99% and the shortage cost for 0 to 0.13%.

5. More conservative ORDCs tend to result in higher fixed cost and this is balanced out by their lower fuel cost. This is particularly the case when comparing the variants with different value of lost load. For example, the 13500/Post-activation/Independent variant incurs 352 k € of fixed cost and 1,304 k € of fuel cost, compared to the 8300/Post-activation/Independent that incurs 343 k € of fixed cost and 1,316 k € of fuel cost .

This last point is further highlighted by the decomposition of the production cost by source of generation and the reliance of some variants on emergency generation. Table 7 presents the decomposition of the flexible production cost as a function of the source of production. There are three categories: CCGTs, OCGTs and emergency generators consisting of turbojet, Non-CIPU generation and foreign balancing capacity. The table shows that conservative ORDCs tend to rely more on CCGTs and less on emergency generation and OCGTs. This difference is clearly visible between the variants that use an Independent distribution compared to their counterparts as well as the variants with VOLL at 13500 compared to their counterparts.

			Prod. cost	CCGT	OCGT	Emerg. gen.
8300	Scheduled B.C.	Independent	1.693	1.497	0.087	0.109
		Correlated	1.697	1.492	0.092	0.114
	Actual B.C	Independent	1.691	1.497	0.087	0.107
		Correlated	1.694	1.492	0.092	0.110
13500	Scheduled B.C	Independent	1.688	1.508	0.079	0.101
		Correlated	1.685	1.503	0.085	0.097
	Actual B.C.	Independent	1.684	1.508	0.079	0.097
		Correlated	1.683	1.504	0.084	0.095

Table 7: Production cost decomposition of the variants by source of generation in millions of euros per day.

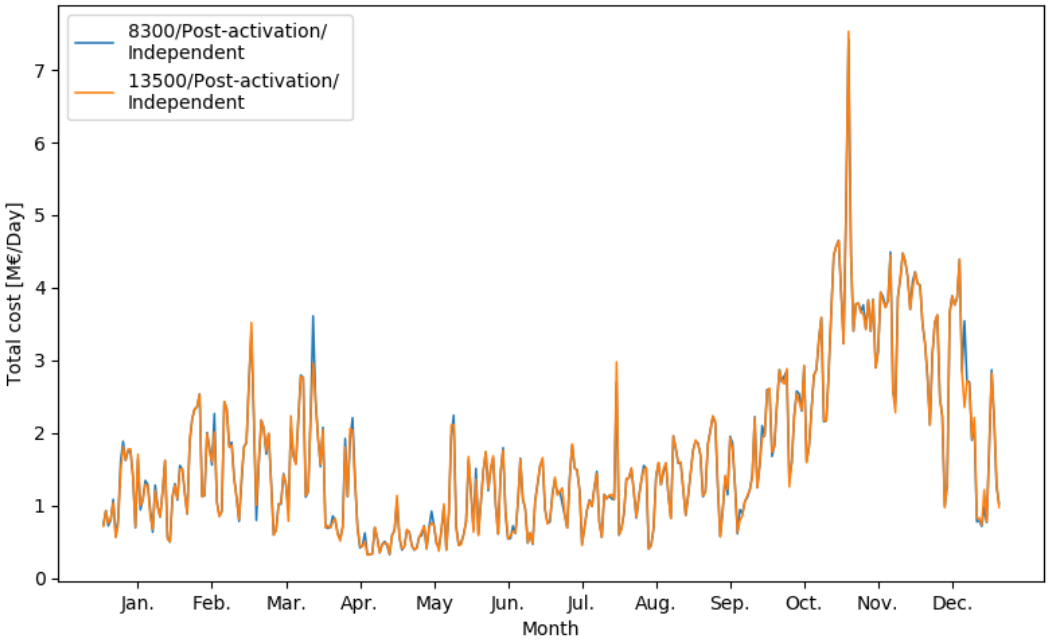

Figure 15: Total cost per day in million euros.

In figure 15 we present the variation of total cost across the days of the year. The total cost of one day can vary from less than 1 M € to more than 7 M €in particularly stressed days. Despite these variations from one day to another, the different variants produce similar total cost. Interestingly, therefore, the performance of the system in terms of cost is quite stable with respect to the ORDC that is implemented.

			Fast reserve adder [€/MWh]	Slow reserve adder [€/MWh]
8300	Pre-Activation	Independent	5.78	0.25
		Correlated	2.86	0.36
	Post-Activation	Independent	5.78	0.14
		Correlated	2.74	0.30
13500	Pre-Activation	Independent	6.50	0.37
		Correlated	3.28	0.56
	Post-Activation	Independent	6.20	0.21
		Correlated	2.92	0.32

Table 8: Mean level of the adders for the reference scenario in euro per MWh.

6.2. Price Analysis of the Reference Scenario

The values of the adders that result from the different variants under the reference scenario are presented in table 8. The fast adder varies from 2.7 € per MWh to around 6.5 € per MWh and the slow adder from 0.15 € per MWh to 0.5 € per MWh. The adders generated by the different variants are thus more significantly dependent on the choice of ORDC than system cost. We can reach the following observations from the table.

1. Conservative ORDCs (13500 variants and Independent variants) produce higher adders than their counterparts. Note that the most significant difference is caused by the distribution of the 7.5-minute imbalance increments, with the independent variants producing fast reserve adders that are approximately twice the value of their counterparts.

2. The pre/post-activation variants behave similarly. Variants with pre-activation capacity yield a higher mean level for the adder, with most of this increase originating from a higher slow reserve adder.

3. Correlated variants result in a higher slow reserve adder. This is driven by the fact that CCGTs have lower incentives for commitment, which decreases the committed balancing capacity and increases the value of the slow adder.

This last point highlights a fundamental difference between the variations in terms of distribution of imbalance increments versus the variations of the VOLL. The independent and correlated variants only impact the 7.5-minute ORDC and increase or decrease the incentives for committing CCGTs, while keeping the slow reserve demand constant. In comparison, variations of the VOLL impact both the 7.5-minute and 15-minute ORDCs.

Table 9 measures the effect on the level of the mean adder from changing one parameter between the different variants. We find that the most impactful change is the distribution of the 7.5-minute imbalance increments. The value of lost load and the pre/post-activation reserve rank second and third in terms of their effect on the adders.

			Fast reserve adder [€/MWh]	Rise in the level of the fast reserve adder caused by a change in a variant [%]		
				8300 to 13500	Sched. to Act. B.C.	Corr. to Ind.
8300	Pre-Activation	Correlated	2.86	15	-4	102
		Independent	5.78	12	0	
	Post-Activation	Correlated	2.74	6		111
		Independent	5.78	7		
13500	Pre-Activation	Correlated	3.28		-11	98
		Independent	6.50		-5	
	Post-Activation	Correlated	2.92			112
		Independent	6.20			

Table 9: Effect of changing one parameter of the variant on the level of the adder.

Figure 16 attempts to quantify the reliability of price signal generated by the ORDC in terms of profitability for owners of flexible assets. The figure compares the price signal obtained by 4 variants, beginning with the most conservative variant that produces the highest adder (13500/Post-activation/Independent) and modifying each of the design parameters in turn. The y-axis displays the mean value of the adder as a function of the risk aversion of the agents on the x-axis. The risk aversion can range from 0% to 100%, where 0% is a completely risk neutral agent and 100% is a completely risk averse one. Depending on the risk aversion α of an agent, the agent will only consider the $100 - \alpha$ worst adders for computing its payoffs from the adder.

We observe a notable drop in the value of the payoff curve for low values of the x axis, which corresponds to the impact of a very high adder resulting from very stressed conditions in the system. These highly stressed conditions constitute less than 1% of the total possible outcomes in the system. It is possible to assess the quality of the signal produced by a variant by analysing the persistence of the adder when the risk aversion increases.

In figure 16, we observe that the correlated variant is the least persistent by a wide margin. The value of lost load and the pre/post-activation capacity produce similar levels of persistence. Note that, for these variants, the decrease can be considered constant until a risk aversion level of 7.5%, which indicates a mean adder that is generated by the repetition of a large number of occurrences of small adders in the market.

Figure 17 confirms the previous observation. This figure shows the percentage of the mean adder that is formed by discrete adders of a particular value. For example, we observe that slightly less than 40% of the mean adder is generated by discrete adders of approximately 100 €/MWh. This figure displays the difference between the pre/post-activation capacity, and it illustrates (i) the higher reliance of pre-activation capacity on extreme adders (more than 2000 €/MWh) and (ii) the higher share of adder between 50 and 100 €/MWh for the post-activation capacity. Even if different variants produce a similar level of mean adder, the distribution of the adders over a year of operations can

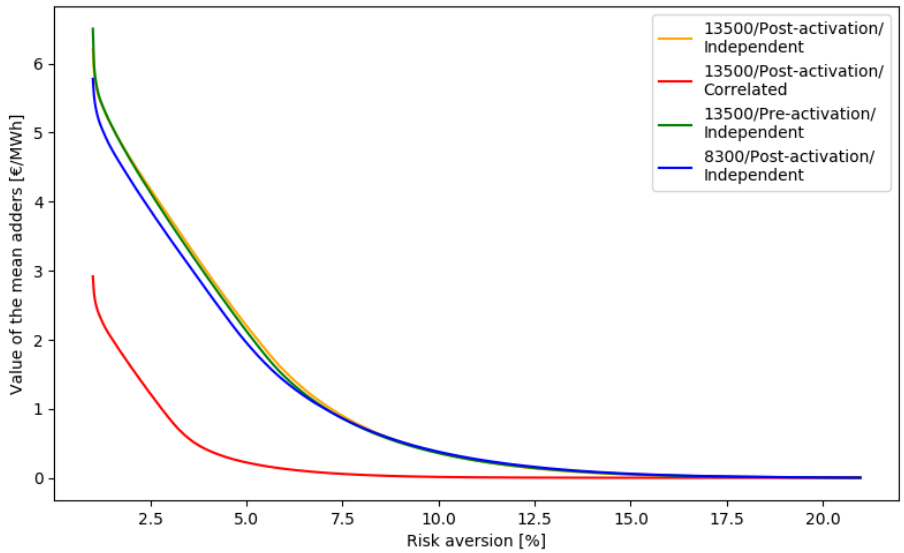

Figure 16: Adder payoff as a function of the risk aversion of the agents.

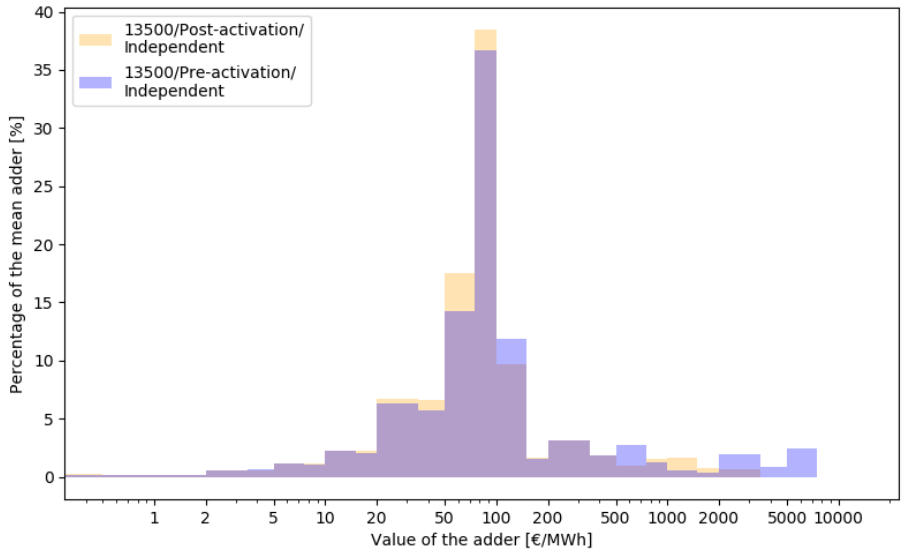

Figure 17: Decomposition of the mean adder by value of the discrete adder[5]

be notably different.

In figure 18 we present the distribution of the adder across the months of the year. The figure only presents the mean price per month for the 13500 variants. We observe that the independent variants are consistently higher than the correlated ones. The pre and post-activation capacity variants are mostly similar, except for July.

This information can also be represented at a resolution of days. Figure 19 presents

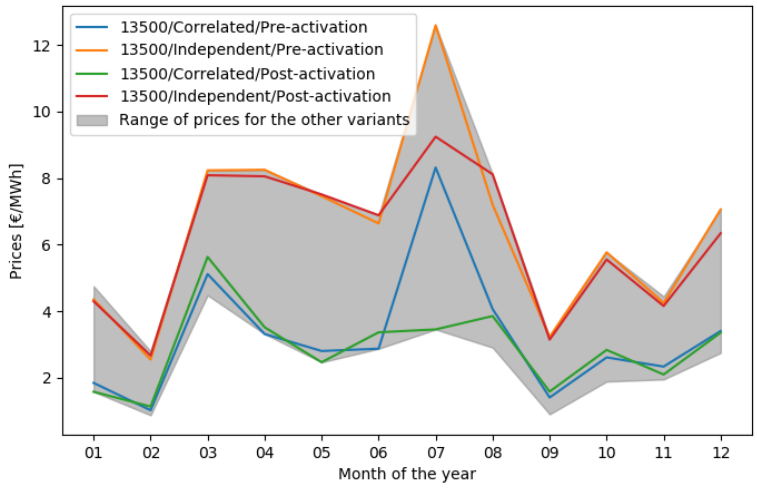

(a) Fast adder

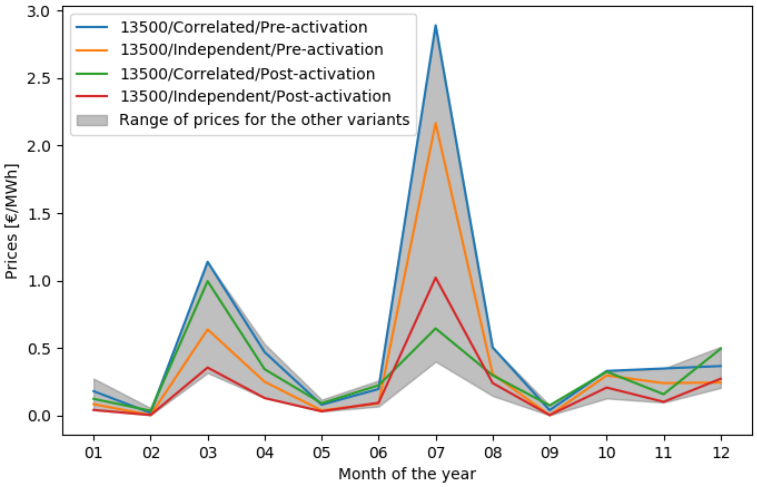

(b) Slow adder

Figure 18: Mean level of adder per month.

the mean fast adder per day for 2018. It shows that the mean price per day is most of the time between 0 and 10 €/MWh, while in approximately 50 days the average adder is higher than 10 € per MWh.

6.3. Shortage Metrics of the Reference Scenario

There are different types of shortage that can occur in the simulator:

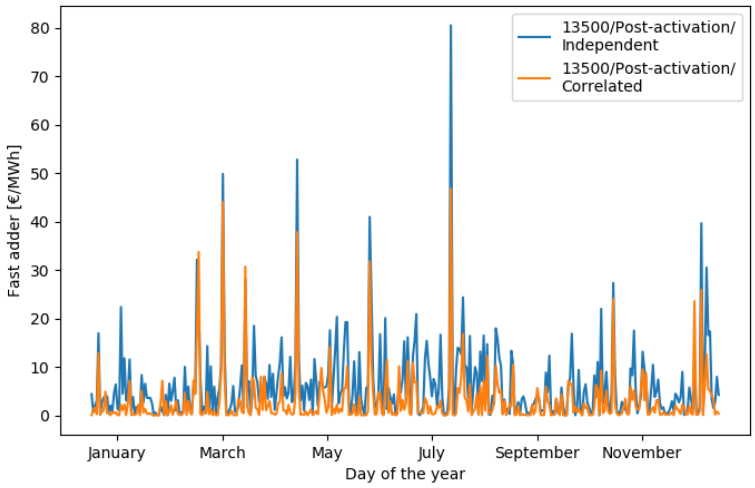

(a) Yearly distribution

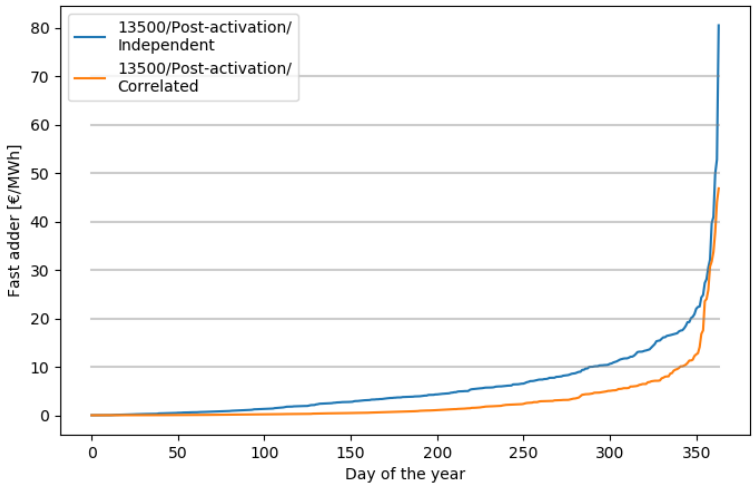

(b) Cumulative distribution function

Figure 19: Mean fast reserve adder per day [€/MWh] for 2018

1. There is an *actual shortage* when the amount of fast reserve is not able to cover the imbalance. In this situation, the value of the adder drops to 0 €/MWh, because the marginal cost of the system rises to the value of lose load.

2. There is a *planned shortage* when it is not economically interesting to activate an expensive emergency generator in order to cover for a small imbalance, even if the

			Actual shortage		Planned shortage		Unplanned shortage	
			ENS [MWh]	LOLE [hour]	ENS [MWh]	LOLE [hour]	ENS [MWh]	LOLE [hour]
8300	Pre-Activation	Independent	51.11	0.38	58.45	2.63	55.73	1.38
		Correlated	4.06	0.25	17.74	3.89	65.22	1.75
	Post-Activation	Independent	0.00	0.00	2.83	2.88	38.56	1.13
		Correlated	4.06	0.25	18.62	4.51	61.83	1.50
13500	Pre-Activation	Independent	10.83	0.13	18.83	2.13	31.25	1.50
		Correlated	59.00	0.75	63.49	2.88	41.48	1.63
	Post-Activation	Independent	2.71	0.13	7.55	2.13	21.51	0.88
		Correlated	10.83	0.13	17.94	3.76	37.65	1.13

Table 10: Energy not served and loss of load expectation under actual shortage, planned shortage and unplanned shortage.

system is not particularly stressed. The remaining capacity margin in the system is not 0 MW, and the adder does not drop to 0 €/MWh.

3. There is an *unplanned shortage* when the behaviour of the economic dispatch, which has no look-ahead, creates a shortage situation. This can occur if the dispatch fails to anticipate the upcoming ramping needs because of the its limited lookahead horizon.

Table 10 presents the shortage metrics for the reference scenario.

6.4. Sensitivity Analysis for the Variation of the Availability of mFRR for the 7.5-Minute ORDC

Allowing a higher availability of mFRR to participate in covering the demand of the 7.5-minute ORDC does decrease the total flexible operating cost, albeit marginally, as indicated in table 11. By increasing this availability, we reduce the need for aFRR from CCGT, and as such decrease the fixed cost of operating the system.

The effects of modifying ρ on the adder are two-fold: increasing ρ (i) reduces notably the level of the fast adder by increasing the fast balancing capacity pool, and (ii) increases marginally the level of the slow reserve adder. Increasing the availability of mFRR for covering the demand the 7.5-minute ORDC reduces the need for aFRR from CCGTs, and has a direct effect on their commitment. This compresses the committed balancing capacity, which in turn increases the level of the slow adder.

Note that our simulator produces higher mean adder than [ELI18] for a similar generation pool. More specifically, the study of ELIA produces a mean adder of 0 to 0.13 €/MWh, depending on the specific assumptions. Instead, our simulator produces a mean adder of 0.74 or 0.81 €/MWh for the variants closest to the ELIA studies (correlated imbalance increments, VOLL at 8300, ρ at 50%). This comparison needs to take

			Total Cost [M€/Day]		
			$\rho = 0\%$	$\rho = 28\%$	$\rho = 50\%$
8300	Pre-Activation	Independent	1.700	1.693	1.691
		Correlated	1.702	1.691	1.688
	Post-Activation	Independent	1.699	1.692	1.687
		Correlated	1.705	1.691	1.687
13500	Pre-Activation	Independent	1.688	1.680	1.680
		Correlated	1.697	1.683	1.683
	Post-Activation	Independent	1.694	1.681	1.679
		Correlated	1.696	1.681	1.684

Table 11: Total cost as a function of ρ, the availability of mFRR for the 7.5-minute ORDC.

F

			Fast reserve adder [€/MWh]			Slow reserve adder [€/MWh]		
			$\rho = 0\%$	$\rho = 28\%$	$\rho = 50\%$	$\rho = 0\$$	$\rho = 28\%$	$\rho = 50\%$
8300	Pre-Activation	Independent	14.65	5.78	1.57	0.12	0.25	0.33
		Correlated	12.88	2.86	0.81	0.19	0.36	0.54
	Post-Activation	Independent	14.62	5.78	1.51	0.08	0.14	0.29
		Correlated	13.33	2.74	0.74	0.14	0.30	0.48
13500	Pre-Activation	Independent	14.76	6.50	1.66	0.25	0.37	0.32
		Correlated	12.92	3.28	0.90	0.27	0.56	0.62
	Post-Activation	Independent	14.91	6.20	1.55	0.09	0.21	0.25
		Correlated	13.12	2.92	0.92	0.17	0.32	0.62

Table 12: Fast and slow reserve price as a function of ρ, the availability of the mFFR capacity for covering the demand of the 7.5-minute ORDC.

into account the differences in the year that is analysed. ELIA [ELI18] computes an adder for 2017, whereas we simulate 2018. Differences between the results can be further explained by the different dispatch and commitment signals sent by the demand for reserve. Another important difference is that the results reported in ELIA [ELI18] are based the ARC, which estimates a reserve capacity that is likely different from that estimated by a simulator that follows an intraday re-commitment driven by an LOLP-based ORDC.

6.5. Sensitivity Analysis on the Variation of aFRR from Abroad

The level of aFRR capacity that is available from abroad has a slight impact on the total flexible cost, as indicated in table 13. Increasing the flexibility of Inter-TSO capacity tends to decrease the total cost, as intuition suggests.

Moving from 0 MW to 25 MW of aFRR capacity from abroad decreases the level of

			Total cost [M€/Day]		
Inter-TSO aFRR			0	25	50
8300	Pre-Activation	Independent	1.697	1.694	1.693
		Correlated	1.701	1.697	1.691
	Post-Activation	Independent	1.696	1.691	1.692
		Correlated	1.699	1.694	1.691
13500	Post-Activation	Independent	1.690	1.688	1.680
		Correlated	1.698	1.687	1.683
	Post-Activation	Independent	1.691	1.684	1.681
		Correlated	1.697	1.683	1.681

Table 13: Total flexible cost as a function of the Inter-TSO aFRR capacity that is available.

			Fast reserve adder [€/MWh]		
Inter-TSO aFRR			0	25	50
8300	Pre-Activation	Independent	6.12	5.78	5.22
		Correlated	3.34	2.86	2.53
	Post-Activation	Independent	6.26	5.78	5.16
		Correlated	3.12	2.74	2.48
13500	Pre-Activation	Independent	6.91	6.50	5.59
		Correlated	3.62	3.28	2.52
	Post-Activation	Independent	6.82	6.20	5.56
		Correlated	3.45	2.92	2.47

Table 14: Fast and slow reserve price as a function of the available Inter-TSO aFRR capacity.

the fast adder by 5% to 15% and from 25 MW to 50 MW of aFRR by 10% to 20%. The sensitivity of this parameter is smaller than the one recorded for the availability of mFRR.

6.6. Sensitivity Analysis with Respect to the Variation of the Expected Additional Fast Demand Response

Increasing the level of fast demand response has a very limited impact on operating cost, as one can observe in table 15. The level of the adder is presented in table 16, and the behaviour is similar to what is observed for the availability of mFRR for covering the demand of the 7.5-minute ORDC. Increasing the fast balancing capacity pool decreases the level of the fast adder and has a tendency to increase the level of the slow adder.

			Total cost [M€/MWh]	
Additionnal fast DR			0	10
8300	Pre-Activation	Independent	1.693	1.693
		Correlated	1.697	1.697
	Post-Activation	Independent	1.692	1.691
		Correlated	1.698	1.694
13500	Pre-Activation	Independent	1.689	1.688
		Correlated	1.698	1.685
	Post-Activation	Independent	1.688	1.684
		Correlated	1.695	1.683

Table 15: Total flexible cost as a function of additional demand response capacity.

			Fast reserve adder [€/MWh]		Slow reserve adder [€/MWh]	
Additionnal fast DR			0	10	0	10
8300	Pre-Activation	Independent	6.13	5.78	0.17	0.25
		Correlated	2.98	2.86	0.32	0.36
	Post-Activation	Independent	6.08	5.78	0.12	0.14
		Correlated	3.00	2.74	0.25	0.30
13500	Pre-Activation	Independent	6.51	6.50	0.22	0.37
		Correlated	3.44	3.28	0.41	0.56
	Post-Activation	Independent	6.45	6.20	0.14	0.21
		Correlated	3.53	2.92	0.36	0.32

Table 16: Fast and slow reserve price as a function of additional demand response capacity.

7. Conclusions and Perspectives

We develop a detailed unit commitment and economic dispatch simulation model of the Belgian power system in order to analyze the effect of different design choices for Operating Reserve Demand Curves on the cost of system operation and the price of aFRR and mFRR capacity. Our simulator attempts to emulate a best-base, fully coordinated operation of the system from the day ahead to real time. We propose four modules that are interleaved and implemented as a rolling horizon optimization:

- The day-ahead unit commitment module commits slow-moving resources and sets pumped hydro targets for real-time operation.
- The intraday module is run four times a day and commits CCGT units.
- The pre-real time module is run before a balancing interval, and activates fast-moving units.

- The real-time module balances the system in real time, twice per balancing interval, and computes ORDC adders.

The goal of setting up this simulation platform is to quantify the tension of incurring large fixed costs for committing flexible resources that can allow the system to operate reliable in real time, versus running the risk of shedding load. It is exactly this tension that an operating reserve demand curve aims to balance, and our simulation framework allows us to arrive at quantitative conclusions regarding design choices related to ORDCs on the basis of system cost and implied prices for reserve services.

We perform a case study using our simulation platform by focusing on the historical data of Belgian system operation for 2018. Our model is populated with detailed data from the Belgian TSO and other data sources, and we propose a clear mapping between the reserve classifications employed by the Belgian TSO and the definition of fast and slow reserve capacity, for each of which we compute a separate ORDC adder. We validate our model by confirming the proximity of the model results to historical data that transpired in the Belgian market in 2018. We then proceed to examine the following design alternatives related to a choice of ORDC:

- VOLL equal to 13500 €/MWh versus 8300 €/MWh
- Imbalance increments within an imbalance interval that are fully correlated versus fully independent, and
- Real-time reserve capacity in the system which corresponds to pre- or post-activation reserve.

Each of these design options has a geometrical intuition in terms of its impact on the shape of the ORDC, as well as an effect on the cost of operating the system and the implies reserve prices.

In addition to the simulation of a reference scenario, we conduct a sensitivity analysis which examines the impact of the following on our results: (i) increased ability of mFRR reserves to contribute to the 7.5-minute adder, (ii) increased inter-TSO aFRR capacity, and (iii) increased demand response capacity.

We arrive to the following main finding from our analysis:

1. The total flexible operating cost for a day is stable, regardless of the chosen variant. It is also stable for the specific generation pool of Belgium that is investigated in or work.
2. The fast adder varies from 2.8 €/MWh to 6.5 €/MWh in the reference scenario. The main driver of the price is the assumption related to the distribution of the 7.5-minute imbalance increments, followed by the value of lost load.
3. The level of the fast adder is sensitive to assumptions about what resources can contribute towards covering the demand of the 7.5-minute ORDC. Note that this sensitivity was already reported in [ELI18].

In future work, we are interested in developing a Monte Carlo simulation model for the Belgian system which draws samples of system uncertainty, instead of relying on historical data. This would allow us to enhance the statistical reliability of our results, by exposing the system to multiple years of hypothetical operation.

A. Omega Adder

In response to the design proposed in [PB20], ELIA has proposed an alternative formulation for the adder [ELI20] which is referred to as the omega adder. This formulation is based on the classic formulation of the ORDC which is proposed in the present report, and can be described as follows for a fifteen-minute period t:

$$\Omega_t = \begin{cases} 0 & \text{if } \lambda^R_{t-1} = 0 \\ 0 & \text{if } MIP_t \leq Voll \\ \lambda^R_t & \text{else} \end{cases} \tag{25}$$

Here, MIP_t is the Marginal Incremental Price in period t and λ^R_t is the value of the fast adder in period t. This adder is described as follows:

$$\lambda^R_t = \frac{1}{2} \cdot (Voll - MIP_t) \cdot LOLP_{7.5}(R^{7.5}_t) + \frac{1}{2} \cdot (Voll - MIP_t) \cdot LOLP_{15}(R^{15}_t) \tag{26}$$

Here, $LOLP_x$ is the probability of shedding load after x minutes and R^x_t is the remaining capacity margin after x minutes in period t.

Notwithstanding the different assumptions regarding the eligibility of the generation pool and its contribution to the remaining capacity margins, the new features brought by the omega adder include:

1. The setting of the omega at zero when the marginal incremental price is higher than the VOLL, and

2. a filtering condition on the omega for reducing its volatility.

The first new feature is in line with the idea of scarcity pricing as characterized by Hogan [Hog13], as long as the MIP reaches the $Voll$ in period of scarcity of energy. The second rule moves away from the original idea and requires a clarification with respect to the definition of 0 €/MWh. The question of what level of adder is considered equal to 0 needs to be addressed. Should we consider any adder below 0.01 €/MWh equal to 0 or should it be lower than 0.0001 or 0.0000001 €/MWh? The influence of the omega adder would depend on this design choice, as indicated in table 17.

We observe that the sensitivity of the Omega can have an impact of 13% to 25%, which amounts to 0.51 to 0.94 €/MWh if the sensitivity is at 1 cent. A plateau is reached at 10^{-5} €/MWh, and from there on the difference between the classic formulation and the Omega adder is negligible.

The effect is less visible on the adder computed with the *historical* (as opposed to simulated) remaining capacity margin of 2018 with a mean fast adder of 0.18 €/MWh and a mean Omega adder of 0.17 €/MWh.

			Fast res. adder [€/MWh]	Omega adder [€/MWh] with varying sensitivity toward 0 €/MWh condition					
				10^{-2}	10^{-2}	10^{-2}	10^{-2}	10^{-2}	10^{-2}
8300	Pre-Activation	Independent	5.78	4.95	5.74	5.78	5.78	5.78	5.78
		Correlated	2.86	2.32	2.81	2.86	2.86	2.86	2.86
	Post-Activation	Independent	5.78	4.84	5.74	5.78	5.78	5.78	5.78
		Correlated	2.74	2.23	2.71	2.74	2.74	2.74	2.74
13500	Pre-Activation	Independent	6.50	5.62	6.50	6.50	6.50	6.50	6.50
		Correlated	3.28	2.47	3.09	3.09	3.09	3.09	3.09
	Post-Activation	Independent	6.20	5.27	6.20	6.20	6.20	6.20	6.20
		Correlated	2.92	2.27	2.92	2.92	2.92	2.92	2.92

Table 17: Value of the Omega adder with different sensitivities on the filtering condition. The results assume $\rho = 0.28$, additional fast demand response at 10 MW, and fast foreign balancing capacity at 25 MW.

B. Cost Function

The cost function of classical generators with variable outputs and variable heat rates can be written as follows for $x = (p, r^F, r^S, u, v, w, s)$:

$$C_g(x) = \underbrace{\int_0^p C^{CO_2} \cdot ER_g + C_g^F \cdot HR_g(x)dx}_{\text{Production cost}} + u_g \underbrace{(Q_g^{NL} \cdot C_g^F)}_{\substack{\text{Minimum load} \\ \text{const}}} + v_g \underbrace{(C_g^{SU} + Q_g^{SU} \cdot C_g^F)}_{\text{Start-up cost}} \tag{27}$$

Here, C^{C0_2} is the price of a ton of CO_2 ([€/Ton]), ER_g is the emission rate ([Ton /MWh]) of the plant, C_g^F is the cost of the fuel ([€/ Gji]), $HR_g(p)$ is the heat rate as a function of the power output of the generator ([Gji/ MWh]), Q_g^{NL} is the minimum load consumption ([Gji]), C_g^{SU} is the start-up cost ([€]), and Q_g^{SU} is the quantity of fuel required for starting up ([Gji]). The parameters for the different CCGT and OCGT units are extrapolated from the real parameters of a private database. This extrapolation is performed in order to adapt our realistic data to capacity levels that are not explicitly represented in our database. The fuel cost is based on the monthly historical spot TTF prices [Ele]. The heat rate is piecewise constant.

C. Example Pre and Post-Activation variants

Imbalances are defined in our analysis as the difference between the scheduled demand ($\tilde{D}$) and the actual demand (D) at the beginning of an imbalance interval.

$$imb = \tilde{D} - D \tag{28}$$

By hypothesis, we assume that the full imbalance is met by the activation of balancing capacity. As such, if we use as reference the real-time reserve after the activation of the

		t_1	t_2	t_3	t_4
Demand forecast	$\tilde{D}$	100	110	130	130
Actual demand	D	95	105	130	135
Imbalance	imb	5	5	0	-5
Reserve before activation	r^{BA}	50	40	20	20
Reserve after activation	r^{AA}	55	45	20	15

Table 18: Evolution of the reserve available for the before and after activation variant

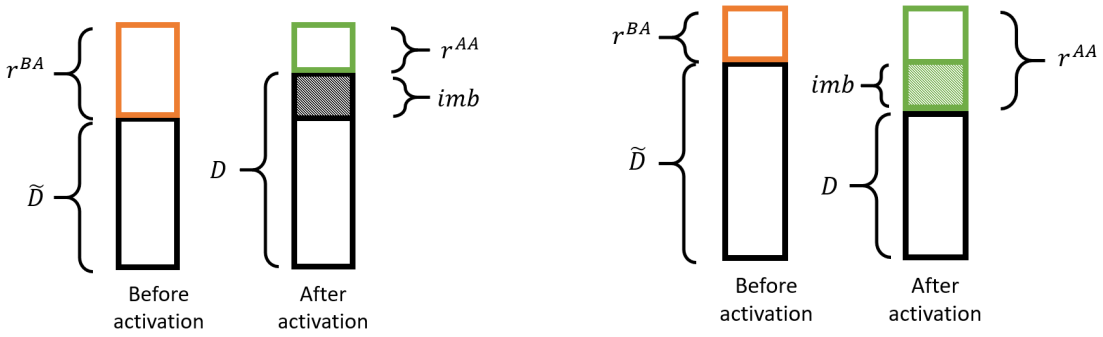

(a) Negative imbalance

(b) Positive imbalance

Figure 20: Before and after activation remaining capacity

balancing capacity, the remaining capacity of both the after-activation variant and the before-activation variant can be defined as follows.

$$r^{AA} = r^{RT}$$
$$r^{BA} = r^{RT} - imb$$

An example of the remaining capacity after and before activation are illustrated by the table 18 on a system with 150 MWh of balancing capacity. The distinction is also illustrated in figure 20. The sign of the imbalances affects the level of the before-activation reserve compared to the level of the after-activation reserve, and this creates a horizontal shift in the ORDC, as indicated by figure 2.

References

[BSB+15] Emmanouil A. Bakirtzis, Christos K. Simoglou, Pandelis N. Biskas, Dimitris P. Labridis, and Anastasios G. Bakirtzis. Comparison of advanced power system operations models for large-scale renewable integration. *Electric Power Systems Research*, 128:90–99, November 2015.

[Dev17] Daniel Devogelaer. Increasing interconnections: to build or not to build, that is (one of) the question(s). Technical report, Federal Planning Bureau, September 2017.

[EE21] ENTSO-E. ENTSO-E Transparency Platform, May 2021.

[Ele] Elexys. Spot-TTF.

[ELI] ELIA. Installed Capacity By Units 2018.

[ELI18] ELIA. Study report on Scarcity Pricing in the context of the 2018 discretionary incentives. Technical report, October 2018.

[ELI19] ELIA. Adequacy and flexibility study for Belgium 2020-2030. Technical report, ELIA, 2019.

[ELI20] ELIA. Preliminary report on Elia's findings regarding the design of a scarcity pricing mechanism for implementation in Belgium. Technical report, September 2020.

[ELI21] ELIA. Data Download Page, May 2021.

[ERC] ERCOT. ERCOT Market Training, ORDC Workshop.

[Hog13] William W. Hogan. Electricity Scarcity Pricing Through Operating Reserves. *Economics of Energy & Environmental Policy*, Volume 2(Number 2), 2013.

[HP19] William W Hogan and Susan L Pope. PJM Reserve Markets: Operating Reserve Demand Curve Enhancements. page 87, March 2019.

[LMSA20] Luke Lavin, Sinnott Murphy, Brian Sergi, and Jay Apt. Dynamic operating reserve procurement improves scarcity pricing in PJM. *Energy Policy*, 147:111857, December 2020.

[NYI19] NYISO. Ancillary Services Shortage Pricing. Technical report, December 2019.

[PB20] Anthony Papavasiliou and Gilles Bertrand. Market Design Option for Scarcity Pricing in European Balancing Markets. 2020.

[PSB17] Anthony Papavasiliou, Yves Smeers, and Gilles Bertrand. Remuneration of Flexibility using Operating Reserve Demand Curves: A Case Study of Belgium. *The Energy Journal*, 38(01), September 2017.

[PSB18] Anthony Papavasiliou, Yves Smeers, and Gilles Bertrand. An Extended Analysis on the Remuneration of Capacity under Scarcity Conditions. *Economics of Energy & Environmental Policy*, 7(2), April 2018.

[PSdMd19] Anthony Papavasiliou, Yves Smeers, and Gauthier de Maere d'Aertrycke. Study on the general design of a mechanism for the remuneration of reserves in scarcity situations. page 90, June 2019.

[PSdMd21] Anthony Papavasiliou, Yves Smeers, and Gauthier de Maere d'Aertrycke. Market Design Considerations for Scarcity Pricing: A Stochastic Equilibrium Framework. *The Energy Journal*, 42(01), September 2021.

[SBB10] Christos K. Simoglou, Pandelis N. Biskas, and Anastasios G. Batirtizis. Optimal Self-Scheduling of a Thermal Producer in Short-Term Electricity Market by MILP. *IEEE Transactions on Power Systems*, 25(4), November 2010.

[SPAK17] H.P. Simao, W.B. Powell, C.L. Archer, and W Kempton. The challenge of integrating offshore wind power in the U.S. electric grid. Part II: Simulation of electricity market operations. *Renewable Energy*, 103:418–431, April 2017.

[ZB14] Zhi Zhou and Audun Botterud. Dynamic Scheduling of Operating Reserves in Co-Optimized Electricity Markets With Wind Power. *IEEE Transactions on Power Systems*, 29(1):160–171, January 2014. Conference Name: IEEE Transactions on Power Systems.

[ZZWT20] J. Zarnikau, S. Zhu, C. K. Woo, and C. H. Tsai. Texas's operating reserve demand curve's generation investment incentive. *Energy Policy*, 137(C), 2020. Publisher: Elsevier.